

AD 670 925

TECHNIQUES FOR FABRICATING SCANNABLE COLD CATHODES

Dietrich Dobischek, et al

Army Electronics Command  
Fort Monmouth, New Jersey

March 1968

AD

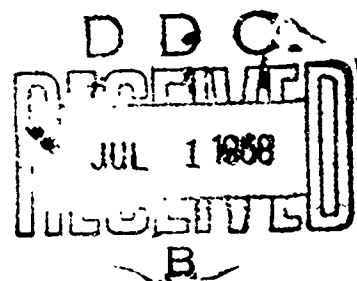
Research and Development Technical Report  
ECOM-2948

TECHNIQUES FOR FABRICATING  
SCANNABLE COLD CATHODES

by

Dietrich Dobischek  
Nelson Dent

March 1968



THIS DOCUMENT HAS BEEN APPROVED  
FOR PUBLIC RELEASE AND SALE; ITS  
DISTRIBUTION IS UNLIMITED.

ECOM

UNITED STATES ARMY ELECTRONICS COMMAND • FORT MONMOUTH, N.J.

Reproduced by the  
CLEARINGHOUSE  
for Federal Scientific & Technical  
Information Springfield Va. 22151

ACCESSION FOR	
OFSTI	WHITE SECTION <input type="checkbox"/>
DOC	BUFF SECTION <input type="checkbox"/>
UNANNOUNCED	<input type="checkbox"/>
JUSTIFICATION	
BY	
DISTRIBUTION/AVAILABILITY CODES	
DIST.	AVAIL. and/or SPECIAL
1	

## NOTICES

### Disclaimers

The findings in this report are not to be construed as an official Department of the Army position, unless so designated by other authorized documents.

The citation of trade names and names of manufacturers in this report is not to be construed as official Government indorsement or approval of commercial products or services referenced herein.

### Disposition

Destroy this report when it is no longer needed. Do not return it to the originator.

Reports Control Symbol  
OSD-1366

TECHNICAL REPORT ECOM-2948

TECHNIQUES FOR FABRICATING  
SCANNABLE COLD CATHODES

by

Dietrich Dobischek  
Nelson Dent

Electron Tubes Division  
Electronic Components Laboratory

MARCH 1968

DA Task No. 1H6-22001-A-055-03

This document has been approved for public release  
and sale; its distribution is unlimited.

U. S. ARMY ELECTRONICS COMMAND, FORT MONMOUTH, NEW JERSEY

### Abstract

#### A. Experiments with Field Emission Type of Cathodes

The formation of asperities has been demonstrated on plain molybdenum layers using the aluminum alloying technique. It was found that too little aluminum fails to produce asperities whereas an excess of aluminum results in irregular corrosion of the molybdenum surface.

Experiments in which asperities were grown on molybdenum areas confined by insulating layers showed that the presence of these layers may affect the formation of asperities. Alumina inhibited the growth of asperities in the immediate vicinity of the alumina layer. Silicon monoxide did not appear to adversely influence the formation of asperities.

#### B. Experiments with Transverse-Field Type of Cathodes

The preparation of transverse-field type of cathodes has been explored using various cathode configurations, materials and techniques.

Vacuum-deposition methods were found to be superior to spray-coating techniques in the preparation of the cathodes.

Cathode configurations in which the gap between the two conductors was controlled by an insulating film sandwiched between the conductors appeared to be the most promising approach toward the fabrication of a useful cathode. Difficulties were experienced with such structures from short circuits between the conducting layers. It was concluded that these failures were not necessarily caused by defects of the insulating layer, but that, in some instances, the two conductors may have come in direct contact inside the structure due to a mismatch of the thicknesses of the insulating layer and the base electrode.

The feasibility of preparing a BaO film such as to carry an electron current across the gap of a cathode structure has been demonstrated.

## CONTENTS

	<u>Page</u>
INTRODUCTION	1
Objective of the Program and Approach	1
DISCUSSION	2
Experimental Setup	2
A. Experiments with Field-Emission Type of Cathodes	2
Arrays of Cathodes	2
Formation of Asperities on Plain Molybdenum Films	3
General Experimental Procedures	3
Substrate Cleaning	3
Substrate Degassing	3
Molybdenum Deposition and Aging	5
Aluminum Deposition and Re-Evaporation	5
Testing of the Samples and Results	6
Formation of Asperities on Molybdenum Within Grooves Formed in an Insulating Layer	8
Formation of Asperities Within Grooves Formed in an Alumina Layer by Masking	8
Formation of Asperities Within Grooves Formed in a Silicon Monoxide Layer by Masking	12
Formation of Asperities Within Grooves Formed in a Silicon Monoxide Layer by Etching	12
B. Experiments with Transverse-Field Type of Cathodes	15
Introductory Remarks	15
Transverse-Field Cathode # 1	15

Transverse-Field Cathodes # 2 through # 5	<u>Page</u> 19
Transverse-Field Cathode # 2	19
Transverse-Field Cathode # 3	21
Transverse-Field Cathode # 4	24
Transverse-Field Cathode # 5	25
Transverse-Field Cathode # 6	33
Transverse-Field Cathodes # 7 and # 8	37
Transverse-Field Cathode # 7	37
Transverse-Field Cathode # 8	39
Transverse-Field Cathodes # 9 through # 11	39
Transverse-Field Cathode # 9	42
Transverse-Field Cathode # 10	44
Transverse-Field Cathode # 11	45
SUMMARY	45
A. Field-Emission Type of Cathodes	45
B. Transverse-Field Type of Cathodes	46
FUTURE PLANS	47
A. Field-Emission Type of Cathodes	47
B. Transverse-Field Type of Cathodes	47
REFERENCES	48
ACKNOWLEDGEMENTS	48

#### FIGURES

1. Furnace	4
2. Asperities Formed on Plain Molybdenum Surfaces	7
3. Molybdenum Surface Corroded by the Use of Excessive Aluminum	9

4.	Asperities Formed on Molybdenum Within Grooves Produced in an Alumina Layer by Masking	Page 11
5.	Asperities Formed on Molybdenum Within Grooves Produced in a Silicon Monoxide Layer by Masking	13
6.	Structure of Transverse-Field Cathode # 1	16
7.	Transverse-Field Cathode # 1: Setup for BaO Deposition	18
8.	Transverse-Field Cathode # 2: Setup for Rotating the Nickel Sleeve	20
9.	Transverse-Field Cathode # 2: Deposition of the Nickel Strips	22
10.	Transverse-Field Cathode # 4: Al <sub>2</sub> O <sub>3</sub> Coated Sleeve Ready for the Deposition of the Nickel Strips (Side View)	26
11.	Transverse-Field Cathode # 4: Side View of the Cathode After Nickel Deposition and Removal of the Masks (Test Circuits are Included)	27
12.	First Version of Transverse-Field Cathode # 5: Nickel Sleeve with Nickel Masks (Top View)	28
13.	First Version of Transverse-Field Cathode # 5: Nickel Sleeve Partially Coated with Al <sub>2</sub> O <sub>3</sub> and Furnished with Contact Strips (Side View)	30
14.	Final Version of Transverse-Field Cathode # 5: Improved Method of Mounting the Sleeve	31
15.	Final Version of Transverse-Field Cathode # 5: Setup for Final Processing and Testing	32
16.	Structure of Transverse-Field Cathode # 6	34
17.	Structure of Transverse-Field Cathodes # 7 and # 8 (Shown Without BaO Coating)	38
18.	Cathode Structure of the Type of Transverse-Field Cathodes # 7 and # 8 with Electrically Shorted Conductors	40
19.	Basic Structure of Transverse-Field Cathodes # 9 through # 11	41
20.	Transverse-Field Cathodes # 9 through # 11: Assembly of the Molybdenum Pellet and the Tantalum Mask	43

## TECHNIQUES FOR FABRICATING SCANNABLE COLD CATHODES

### INTRODUCTION

#### Objective of the Program and Approach

The objective of the program is to fabricate an array of scannable micron-sized cathodes to be used in combination with a phosphor screen as a novel display device. Two approaches toward the preparation of the cathodes are being pursued.

In one approach, tiny asperities are grown at the surface of molybdenum metal inside a micron-sized cavity produced in an insulating film. The asperities serve as field emitter tips from which field emission may be drawn by applying a voltage to a molybdenum film deposited on the top of the insulating layer.

To fabricate a scannable array of such cathodes, a series of parallel molybdenum strips is deposited onto a highly refractory substrate. A thin film of aluminum oxide is evaporated onto the molybdenum strips and another set of parallel molybdenum strips is deposited on the aluminum oxide in a direction perpendicular to that of the base molybdenum strips. Using polystyrene balls of 1/4-micron diameter as masking material during the deposition of the top molybdenum strips, tiny holes have been created in the strips. The sample is then etched in hot, concentrated orthophosphoric acid. This treatment removes the aluminum oxide from the places where it is not covered by the top molybdenum strips. Underneath these strips, the aluminum oxide is etched away where the tiny holes were created in the strips during deposition. At these spots, small cavities are formed in the aluminum oxide. At each crossing of a molybdenum top and base strip, bare molybdenum is exposed at the bottom of the cavities. Deposition of a very thin aluminum film on the sample followed by removal of the aluminum by a heat treatment produces tiny asperities on the molybdenum. The asperities formed in the cavities on the bare molybdenum at the bottom represent the field emitter tips previously mentioned. The total number of cavities present in the aluminum oxide at a crossing of a top and base molybdenum strip constitute one individual cathode of the array. Scanning of the cathodes is accomplished by connecting one base molybdenum strip to ground and applying a voltage of 10 to 50 volts between one top molybdenum strip and ground.

The second approach toward the fabrication of the scannable cathodes uses the so-called transverse-field emitter described by D. V. Geppert and B. V. Dore.<sup>(1)</sup> In this cold cathode structure, a narrow gap between two conductors is bridged by a thin film of a semiconductor, e.g. BaO. When a sufficiently high electric field is established between the two conductors, a current passes through the semiconductor. By applying an external accelerating field while operating the device in vacuum, a portion of this current can be drawn into the vacuum.

In the practical construction of the cathodes, the gap between the two conductors may be defined by a thin insulating layer. The semiconductor film is applied to the edge of the structure. If the edge forms the wall of a hole etched into a metal-insulator-metal sandwich a scannable array of the

cathodes can be fabricated in a manner very similar to that described for the construction of arrays of the field-emitter type of cathodes. The only change to be made consists in eliminating the step of growing the asperities inside the cavities and, instead, evaporating a semiconductor film onto the sample. This film forms the desired semiconducting bridge between top and bottom conductor inside each cavity. By applying a voltage across the two conductors, a current may be drawn through the semiconductor. A portion of the electrons may be extracted into the vacuum and accelerated toward a phosphor screen by means of a positive grid electrode mounted in front of the cathode panel.

## DISCUSSION

### Experimental Setup

An efficient double-bell jar VacIon pump system was used in the preparation of the various cathode samples. This vacuum system was a modified version of the pump station described in detail in Technical Report ECOM-2718<sup>(2)</sup>. The original pump station consisted of a 400 L/S VacIon pump combined with a titanium sublimation pump, a rotary oil pump as forepump and a bakeable molecular sieve in the forepump line for trapping back-streaming oil vapors. As new features, a 140 L/S VacIon pump with built-in titanium sublimation pump was added to each of the two bell jar stations. In addition, the molecular sieve was replaced by an efficient liquid nitrogen trap with a by-pass line. The use of the 140 L/S VacIon pumps considerably reduced the pump-down time of the bell jar stations. The liquid nitrogen trap eliminated the need for the periodic bakeout of the molecular sieve and was also considered as a more effective trap since the molecular sieve could not be cooled.

The techniques and the auxiliary equipment used for assembling the experimental setups in the bell jars were the same as those described in Technical Report ECOM-2718<sup>(2)</sup>.

#### A. Experiments with Field-Emission Type of Cathodes

##### Arrays of Cathodes

Initially, attempts were made to fabricate a relatively large-size sample consisting of an array of 16 cathodes formed on a ceramic disc, 1 3/8" in diameter. The large size of the sample complicated the experimental procedures. In particular, the necessity of heating the sample to the high temperatures (1100° to 1200° C) required for the bakeout and the re-evaporation of the aluminum presented problems. In addition, difficulties were experienced in the construction of a reliable mechanism for the necessary transport of the sample to various positions inside the bell jar without breaking the vacuum. Solving these strictly technological problems proved to be rather time-consuming and, therefore, impractical at this early stage of the project. It was therefore decided to discontinue the work on large-size samples and, instead, to explore one particular problem area in the preparation of field-emission type of cathodes, i.e. the process of asperities formation. Consequently no sample arrays were actually fabricated to the point of completion by this technique.

## Formation of Asperities on Plain Molybdenum Films

### General Experimental Procedures

To get acquainted with the basic technique for forming asperities a simple experimental procedure was chosen. First, a molybdenum layer was deposited onto a small sapphire substrate. The molybdenum layer was then coated with a thin film of aluminum and finally the aluminum was removed by evaporation. Specifically, the experimental procedures were as follows:

#### Substrate Cleaning

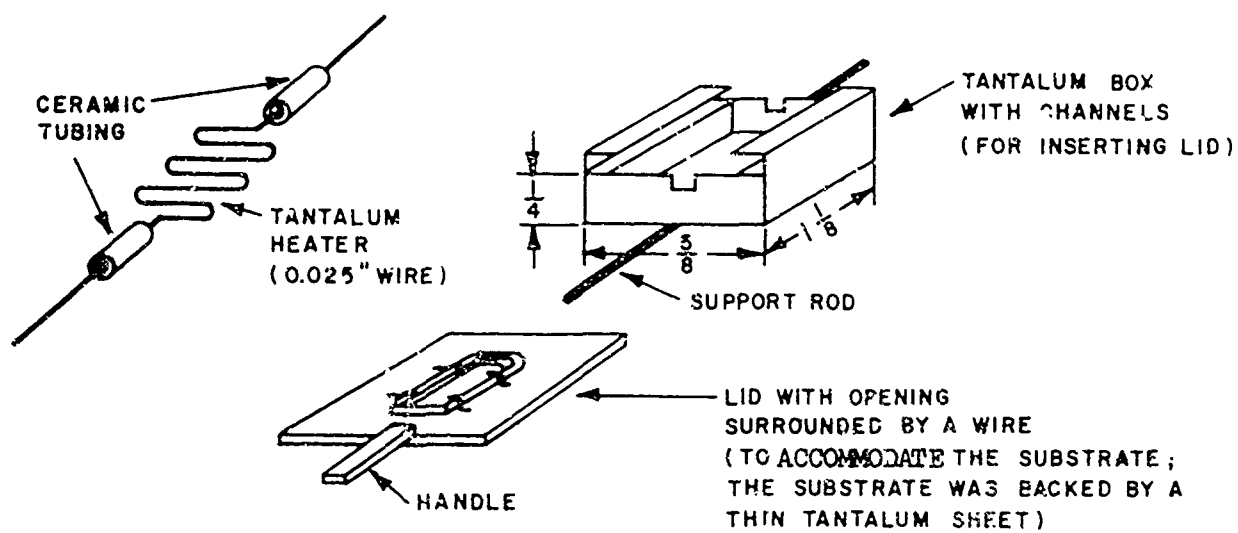
The sapphire substrate (approximately 3/8" wide, 7/8" long, and 1/32" thick) was thoroughly cleaned by scrubbing with a paste of reagent-grade calcium carbonate and distilled water, followed by rinsing with distilled water, a dip in concentrated acetic acid and re-rinsing in distilled water. The final wash in distilled water was assisted by ultrasonic agitation. Subsequently, the substrate was rinsed with filtered distilled water and with methanol, and finally dried in clean air.

#### Substrate Degassing

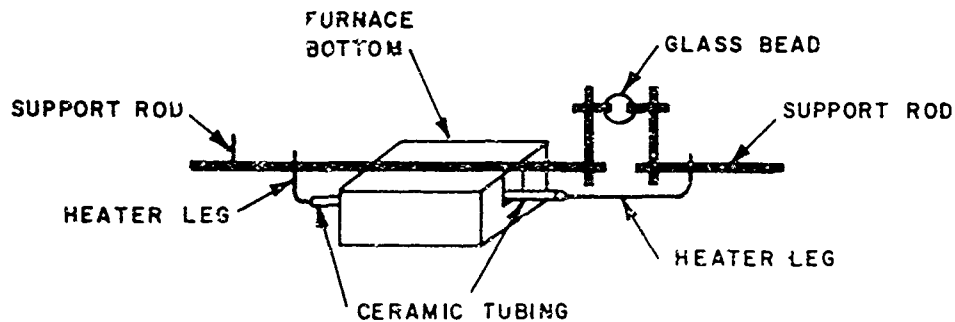
The clean substrate was attached to a small furnace and degassed by gradually heating furnace and substrate to temperatures ranging from 1100° to 1200°. The furnace that proved to be most practical and the mounting of the furnace are sketched in Figure 1. Currents of approximately 17 amperes at voltages around 11 volts were required to obtain the quoted temperatures.

Initially measurement of the substrate temperature by thermocouples (chromel-alumel and Pt/Pt-Rh) was tried with the thermocouple weld either pressed against the substrate or welded to the furnace in close vicinity to the substrate. Both methods were unsatisfactory. In the first method, it was impossible to maintain a sufficiently intimate contact between thermocouple weld and substrate. In the second method, erroneous readings were obtained, probably due to alloying of the thermocouple with the furnace material. To eliminate these problems the temperature readings were finally taken by an optical pyrometer focused on the body of the furnace. The measured data, therefore, only approximate the temperature of the substrate.

The degassing schedule varied in the experiments. In the early runs, the furnace and substrate were raised to the maximum temperature within about one hour and with only forepump vacuum ( $5 \times 10^{-3}$  torr) established in the bell jar. The pressure was then reduced to the  $10^{-6}$  torr range within 1/2 to 1 hour while the furnace temperature was maintained at the maximum level. In the later experiments, the degassing was performed entirely in the low pressure range using heat-up periods of 30 to 45 minutes and keeping furnace and substrate at the maximum temperature for a period of 10 minutes.



#### a. EXPLODED VIEW



#### b. METHOD OF MOUNTING THE FURNACE

FIGURE 1. FURNACE

### Molybdenum Deposition and Aging

The deposition of the molybdenum onto the substrate was carried out using an electron gun (E-gun) as heat source. The substrate was kept at approximately 600° C and was protected by a removable shield prior to the deposition of the molybdenum. The molybdenum was evaporated from pellets, 3/16" thick and 1/4" in diameter. The molybdenum had the tendency to "spit" before melting. When the pellet was slowly heated to the point where the surface began to melt, and the pellet was then allowed to cool before the final evaporation was attempted, the danger of spitting was reduced to a minimum.

The distance between E-gun and substrate varied between 4" and 5 1/2", but in most of the experiments was 5". The molybdenum was usually deposited with the vapor striking the substrate perpendicularly. Occasionally, the substrate was mounted sideways from the E-gun so that the vapors arrived at the substrate under an angle of about 30° from the normal.

The pellet temperatures measured at the beginning of the molybdenum evaporation were approximately 1900° to 2000° C. The bombarding currents ranged from 70 to 120 mA at the fixed initial bombarding voltage of 4 kV. The deposition was usually completed within 30 to 60 minutes. The pressure in the bell jar was in the  $10^{-6}$  torr range.

The deposition of the molybdenum was monitored by an oscillating quartz crystal (cf. Technical Report ECOM-2718 for further detail). The heat generated in the vicinity of the furnace and substrate did not permit the use of the combined crystal and oscillator unit inside the bell jar. Only the crystal was therefore mounted near the substrate and the oscillator placed outside the bell jar. Although the connecting cable was short this arrangement resulted in a considerably reduced reliability of operation. Temperature effects continued to create problems. Some improvement was achieved by mounting the crystal on a water-cooled head, but the data obtained are still considered as only crude approximations. The changes in frequency measured at the end of the molybdenum depositions ranged from 5 to 10 kHz corresponding to estimated film thicknesses of 1000 to 2000 Å.

Immediately upon completion of the deposition, the molybdenum layer was aged by gradually heating furnace and sample to the temperature at which the degassing of the substrate had been performed. Furnace and sample were maintained at this temperature for several minutes and then allowed to cool. The pressure in the bell jar at the end of the aging while the furnace was still operating was approximately  $1 \times 10^{-6}$  torr.

### Aluminum Deposition and Re-Evaporation

The aluminum (high-purity grade, 99.999) was deposited onto the molybdenum layer using a prefired conical basket made from alumina-coated tungsten wire as heating source. Prior to the deposition, the basket with the aluminum and the furnace carrying the sapphire substrate with the molybdenum layer were degassed. The outgassing procedure finally adopted was as follows: First, the tungsten basket with the aluminum was heated to about 1000° C within 20 to 25 minutes while the furnace with the sample

remained at room temperature in order to prevent the molybdenum layer from gettering material generated from the tungsten basket during its degassing. The pressure in the bell jar was at this stage in the lower  $10^{-6}$  torr range. The furnace with the sample was then heated to about  $1150^{\circ}$  C within 30 to 5 minutes. During this period, the temperature of the tungsten basket was at  $900^{\circ}$  to  $1000^{\circ}$  C. Finally, the furnace temperature was reduced to approximately  $600^{\circ}$  C and the deposition of the aluminum was initiated by raising the basket temperature to about  $1150^{\circ}$  and dropping the shutter that had shielded the sample from the tungsten basket during the degassing. Only half of the sample area was coated with aluminum. The other half was masked by a tantalum sheet to provide an untreated molybdenum surface as reference area. The bell jar pressure during the deposition of the aluminum was in the neighborhood of  $1 \times 10^{-6}$  torr.

In monitoring the thickness of the aluminum films by the quartz crystal method the same problems were encountered as in the control of the molybdenum film thickness. The same caution in the interpretation of the data is therefore indicated. With one exception, the changes in frequency ranged from 0.5 to 1 kHz corresponding to estimated film thicknesses of 400 to 800 Å. In the exceptional case, the aluminum was deposited to a considerably larger thickness, approximately 2500 Å (measured frequency change 3.1 kHz). The time of deposition in most of the experiments was 4 to 15 minutes. In one experiment, however, 25 minutes were needed to form an aluminum film only 400 Å thick (0.5 kHz frequency change).

The distance between tungsten basket and sample was, in general, 4". Only during the deposition of the very heavy aluminum film was this distance 5".

The re-evaporation of the aluminum was performed either immediately following the deposition of the aluminum films or, in two experiments, after exposure of the sample for 20 minutes to air of atmospheric pressure and room temperature. In general, the aluminum was evaporated by gradually raising the furnace with the sample to a temperature of  $1150^{\circ}$  to  $1200^{\circ}$  C and maintaining this temperature for 20 to 25 minutes. In the experiment in which the very heavy aluminum film was applied to the molybdenum, the maximum furnace temperature was about  $1260^{\circ}$  and the heating of the sample was continued at this temperature for 65 minutes. The pressure at the end of the aluminum re-evaporation was usually in the lower  $10^{-6}$  torr range.

#### Testing of the Samples and Results

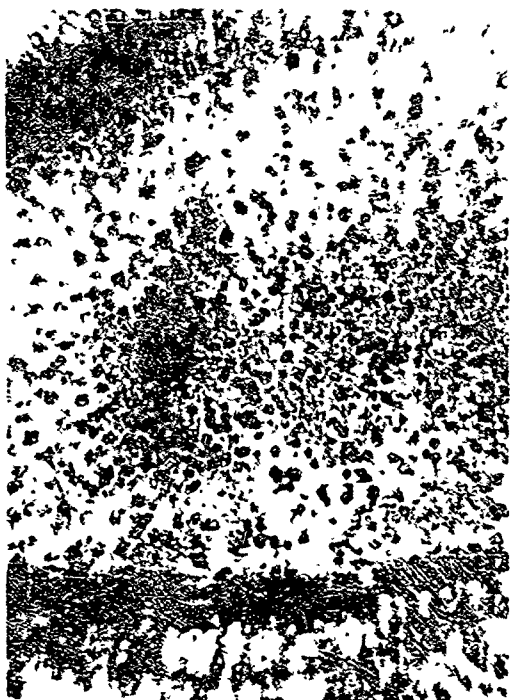
The samples were examined under the microscope in reflected light. Of the six samples prepared, four samples showed the expected formation of asperities in the aluminum treated area. Photographs taken of these samples are displayed in Figure 2 a through d. Differences in the size and density of the asperities will be noticed. The small number of experiments does not permit an explanation of these differences. A more systematic investigation of the numerous factors which may have caused the variations would be necessary.



a.



b.



c.



d.

FIGURE 2. ASPERITIES FORMED ON PLAIN MOLYBDENUM SURFACES

Of the two samples that failed to demonstrate the formation of asperities, the surface of one sample was not changed at all by the aluminum treatment. The aluminum was deposited onto this sample until the frequency change of the quartz crystal was approximately 0.5 kHz. This value was the lower limit for the thickness of the aluminum films applied in the experiments. Application of an insufficient amount of aluminum could therefore be held responsible for the absence of asperities on the sample. However, among the samples prepared, there was another one for which the frequency change during the aluminum deposition was also 0.5 kHz, and this sample did display the characteristic growth of asperities. Because of this fact, it is felt, however, that a faulty aluminum deposition could very well be the reason for the negative result obtained on the one particular sample. This sample was prepared in the experiment previously mentioned in which the exceptionally long deposition time of 25 minutes was required to form the very thin aluminum film on the molybdenum. The reasonable assumption may therefore be made that, as a consequence of the slow deposition, considerable oxidation of the aluminum took place and, hence, too little metallic aluminum was available to promote the growth of asperities. In addition, the presence of excessive aluminum oxide may have been harmful.

A photograph of the surface of the second sample in which the aluminum treatment did not produce a satisfactory result is shown in Figure 3. As can be seen, the sample did not display distinct asperities, but had a non-uniform, corroded appearance. This sample was the one in which the very heavy aluminum film of approximately 2500 Å was applied to the molybdenum. It was therefore concluded that excess of aluminum has caused the observed corrosion of the molybdenum surface.

#### Formation of Asperities on Molybdenum Within Grooves Formed in an Insulating Layer

Work performed at Stanford Research Institute on the formation of asperities (3) met with difficulties when an attempt was made to grow the asperities inside small, micron-size cavities etched through an alumina film on a molybdenum base. No conclusive explanation for the failures was evident. Since it was felt that the experiments described in the preceding paragraphs had provided sufficient experience in the production of asperities on plain molybdenum films, it appeared reasonable to expand the investigations by exploring the aspects of forming the asperities on molybdenum areas confined by insulating layers. To simplify the experimental procedures and the evaluation of the results it was decided not to immediately attempt the growth of asperities at the bottom of micron-size holes, but to produce the asperities inside relatively wide grooves formed in the insulator.

#### Formation of Asperities Within Grooves Formed in an Alumina Layer by Masking

In the first experiment, vapor-deposited alumina was used as the insulator layer. The molybdenum base layer was prepared in essentially the same way as described previously in this report. Also the dimensions of the sapphire substrate were the same as in the earlier experiments. To produce the grooves in the alumina layer the molybdenum film was masked by a nickel grid with a wire diameter of about 12 mils. To insure better contact

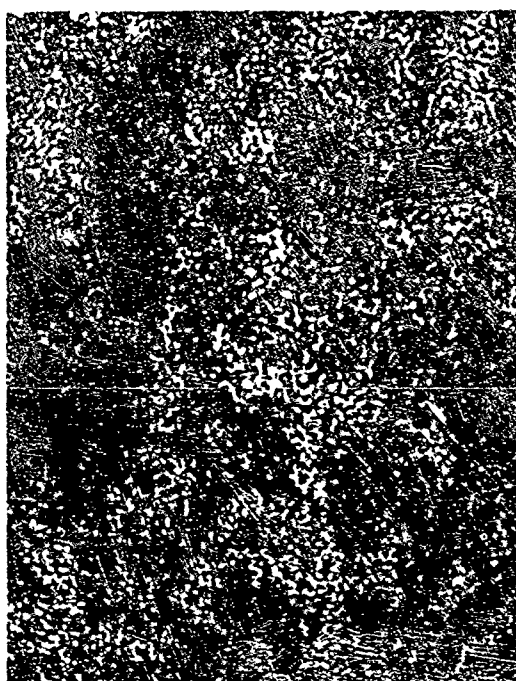


FIGURE 3

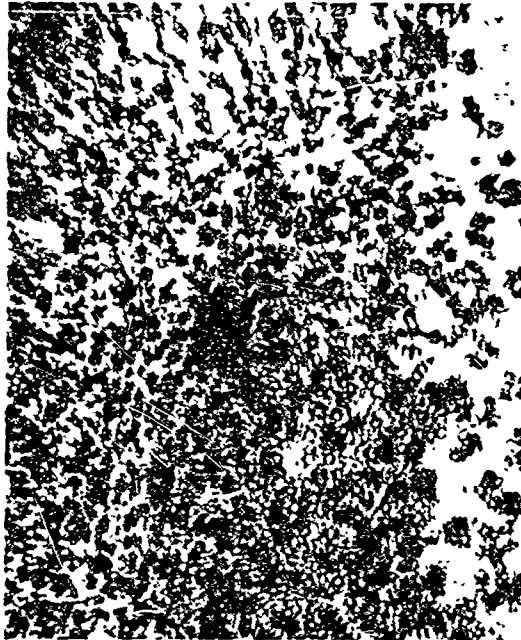
MOLYBDENUM SURFACE CORRODED BY THE  
USE OF EXCESSIVE ALUMINUM

with the molybdenum the nickel grid was flattened in a vise. A pellet, 5/8" in diameter and 1/4" thick, of a "green" (unfired) alumina ceramic (99.5%  $\text{Al}_2\text{O}_3$ ) served as the alumina source and was heated by an E-gun. The distance between the alumina pellet and the substrate with the molybdenum film was approximately 3 1/2". The alumina pellet was slowly degassed by raising the temperature to about 2300° C. At this temperature, the alumina deposition began as indicated by the monitoring quartz crystal. The shutter that had shielded the molybdenum layer during the degassing of the alumina was removed and the alumina deposited through the grid mask onto the molybdenum. The substrate with the molybdenum was kept at about 600° C during the alumina deposition. The deposition was continued until the frequency of the oscillating quartz crystal had changed by approximately 25 kHz. This frequency change corresponds to an estimated film thickness of the order of 1 micron, but this value represents only a lower limit since the quartz crystal was about 2" farther away from the alumina source than the substrate with the molybdenum layer. The duration of the alumina deposition was about 20 minutes. The maximum temperature measured on the alumina pellet was 2380° C. The bell jar pressure was about  $5 \times 10^{-6}$  torr. The alumina deposit was briefly aged by heating at an estimated temperature of 800° C for a period of 20 minutes.

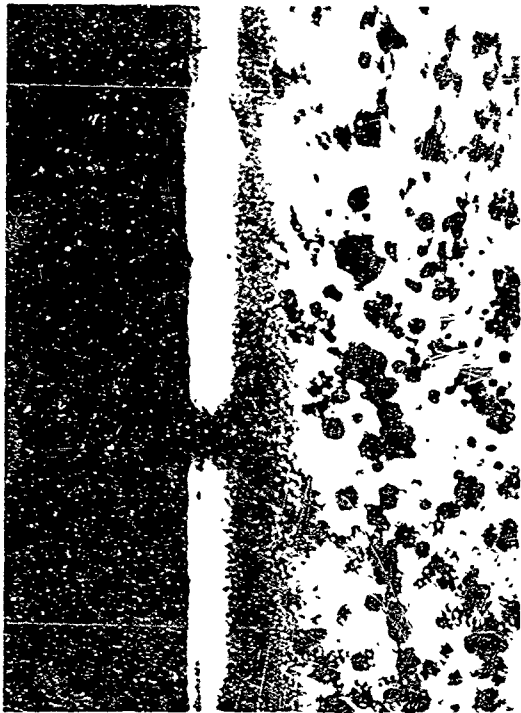
After removal from the bell jar and detachment of the grid mask, the sample was examined. The alumina layer had a dark-brown color. Apparently, partial decomposition of the alumina had occurred during the bombardment with the electron beam and the partial oxygen pressure in the bell jar was too low to cause re-oxidation. The molybdenum underneath the mask had remained bright and shiny.

The aluminum treatment of the sample followed, in general, the schedule used in the experiments with plain molybdenum films.

Examination of the finished sample under the microscope revealed the growth of asperities in the grooves, but the density decreased from the middle of the grooves toward the edges. In close vicinity to the alumina, hardly any asperities were formed. Some isolated, larger specks were noticed along these borderlines. Figures 4a and 4b are presented as examples of the observations. Figure 4a shows a photograph of a molybdenum area located mainly in the middle of a groove. Toward the right-hand side of the picture, the molybdenum area approaches the edge of the groove and the decrease in the density of the asperities can be seen. Figure 4b represents a photograph of a molybdenum area (on the right-hand side of the picture) close to the adjacent alumina layer (black area on the left-hand side). It will be noticed that in the immediate vicinity of the alumina a strip of the molybdenum area has remained apparently unchanged. Considering that the width of this strip (10 to 15 mm in the picture) corresponds in reality to 25 to 40 microns, it is understandable that the formation of asperities inside micron-size holes presents difficulties. A valid explanation for the suppressed growth of the asperities in the vicinity of the alumina cannot be offered at the present time, but would be of vital interest for the solution to the problem.



a.



b.

FIGURE 4. ASPERITIES FORMED ON MOLYBDENUM WITHIN GROOVES PRODUCED IN AN ALUMINA LAYER BY MASKING

#### Formation of Asperities Within Grooves Formed in a Silicon Monoxide Layer by Masking

In order to explore whether other insulators than alumina may show a detrimental effect on the formation of the asperities on molybdenum, the next experiment was performed using silicon monoxide (SiO) instead of alumina as the insulator layer. A minor change was made in the preparation of the molybdenum base layer inasmuch as the molybdenum pellet was outgassed before the furnace with the substrate was degassed.

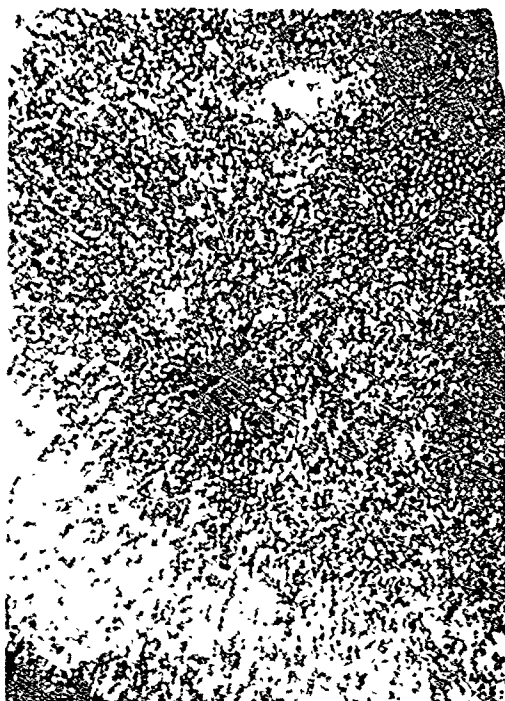
The SiO was evaporated from an alumina-coated tungsten basket. Prior to the evaporation, the SiO had been degassed by raising the basket temperature to 1300° C within 35 minutes and continuing the outgassing at 1050° to 1100° for about 15 minutes. The SiO was deposited through the same nickel grid mask used in the previous experiment. The furnace with the molybdenum-coated substrate was kept at about 600° C during the deposition. The distance between the SiO source and the substrate was approximately 4". The SiO was evaporated at a basket temperature of about 1400° C. The deposition was carried out over a period of 40 minutes. The frequency change of the monitoring quartz crystal was approximately 11 kHz corresponding to an estimated film thickness of about 1 micron. The bell jar pressure was initially in the low  $10^{-7}$  torr range, but increased by an order of magnitude toward the end of the deposition. Immediately upon completion of the deposition, the SiO layer was aged for 35 minutes at a furnace temperature of about 600° C and the aging continued for another 35 minutes at a furnace temperature of approximately 800° C.

The final aluminum treatment of the sample was performed following essentially the same procedures used in previous experiments. It should be noted, however, that the time required in the present experiment for the deposition of the aluminum film was extremely short (2 minutes) although, according to the measured change in frequency (1 kHz), the film was one of the thickest films applied in the normal aluminum treatments. (The deposition time in normal aluminum treatments varied between 4 and 15 minutes.)

The finished sample was examined under the microscope and it was found that asperities had been formed across the entire width of the grooves. The asperities were quite uniform in size and distribution (very small and dense) as can be seen from Figure 5a which shows a photograph taken from a molybdenum area in the middle of a groove. Figure 5b represents a photograph taken near the edge of a groove. The lower part of the picture shows the groove area with the asperities. The upper part of the picture shows the SiO area which exhibited a coarser, reddish grain structure interspersed with finer, whitish spots. As can be noticed in Figure 5b, an especially shiny, narrow strip with a peculiar texture had developed along the edges of the grooves.

#### Formation of Asperities Within Grooves Formed in a Silicon Monoxide Layer by Etching

In the fabrication of an array of scannable cathode, the cavities in the insulator have to be produced by etching. An attempt was therefore made to form asperities inside grooves etched into an insulating



a.



b.

FIGURE 5. ASPERITIES FORMED ON MOLYBDENUM WITHIN GROOVES  
PRODUCED IN A SILICON MONOXIDE LAYER BY MASKING

layer. SiO was selected as the insulator because of the favorable result obtained with this material in the experiment in which the grooves were formed in the SiO by a masking technique. Essentially the same procedure as in this experiment was used for preparing the molybdenum base layer. However, the SiO was evaporated in the present experiment by an E-gun and no mask was attached to the base layer during the deposition of the SiO. The substrate with the molybdenum base layer was briefly outgassed before the SiO was deposited. During the SiO deposition, the furnace with the sample was kept at about 600° C. The distance between the sample and the E-gun was approximately 5". It was necessary to continue the deposition for a period of 50 minutes to form a SiO layer of about 0.6-micron thickness although the final temperature of the SiO was as high as 1550° C and a reasonably low pressure (upper 10<sup>-7</sup> torr range) prevailed in the bell jar. For the deposition of relatively thick SiO layers, the use of the E-gun as heat source was therefore considered as impractical and inferior to the use of a tungsten basket. The relatively small beam area and the limitation in the shifting of the beam appeared to be the reason for the inefficient evaporation of the SiO. After completion of the deposition, the SiO layer was aged by heating for 20 minutes between 700° and 800° (pressure: 6 to 7 x 10<sup>-7</sup> torr).

To form the grooves in the SiO layer by etching, a resistive material had to be applied to the SiO surface to protect the areas that should not be attacked by the etch. This masking layer was produced by depositing molybdenum onto the SiO surface through the same nickel mesh grid used in the previous experiments. Before depositing the molybdenum, the source material (the usual molybdenum pellet) was outgassed at about 1900° C and, subsequently, the furnace with the sample was degassed by raising the furnace temperature to about 1200° C within a period of 35 minutes. The evaporation of the molybdenum was performed at a maximum pellet temperature of about 2100° C and at a bell jar pressure of 8 x 10<sup>-7</sup> torr. Unfortunately, the quartz crystal failed to operate. From the duration of the deposition (50 minutes) and the clouding of the bell jar walls, the final thickness of the molybdenum deposit was estimated to be within the range of thicknesses (1000 to 2000 Å) that were normal for the molybdenum layers prepared in the various experiments. The molybdenum deposit was finally aged by raising the furnace temperature within 25 minutes to about 900° C.

Upon removal of the nickel grid mask, the sample displayed a shiny grid pattern whereas the square molybdenum patches had a dull appearance. Neither with the naked eye nor under the microscope could the presence of SiO be detected where the mesh grid had covered the SiO. When immersed in hydrofluoric acid (H<sub>2</sub>F<sub>2</sub>) the sample failed to show the characteristic behavior of vacuum-deposited SiO layers. Normally, these layers are partially attacked by H<sub>2</sub>F<sub>2</sub> due to the presence of some silicon dioxide (SiO<sub>2</sub>). As the result, the SiO layers are loosened and float away. No such reaction was observed on the sample. There were two possible explanations for the absence of this reaction: (1) The temperature at which the sample with the nickel grid attached had been degassed was quite high (1200° C). The SiO might have been lost, therefore, during this heat treatment either by re-evaporation or, more likely, by chemical reaction with the nickel grid; (2) The SiO did not contain a sufficient quantity of SiO<sub>2</sub> to be visibly attacked by the H<sub>2</sub>F<sub>2</sub>. The second possibility was checked by adding a drop of nitric acid to the H<sub>2</sub>F<sub>2</sub> to induce the formation of SiO<sub>2</sub> thereby making the SiO layer more susceptible to the

attack by the  $\text{H}_2\text{F}_2$ . Unfortunately, the acid mixture instantaneously dissolved the entire coating including the molybdenum layers. Because of this rapid reaction, it was impossible to decide whether or not  $\text{SiO}$  was present. The resultant destruction of the sample terminated the experiment.

It has been learned from the experiment that, after deposition of the  $\text{SiO}$  layer, heat treatments of the sample should be carried out only at moderate temperatures. To minimize the danger of a reaction of the  $\text{SiO}$  with the grid mask, this mask should be made from a more refractory metal than nickel (for instance tantalum). It may be also useful to perform the aging of the  $\text{SiO}$  layer in a rather poor vacuum ( $10^{-2}$  to  $10^{-3}$  torr) to promote oxidation of the  $\text{SiO}$ .

## B. Experiments with Transverse-Field Type of Cathodes

### Introductory remarks

The basic structure of the transverse-field cathode has been described in the introduction to this report. In essence, the cathode consists of two conductors separated by a narrow gap that is bridged by a thin film of a semiconductor. To test the performance of a cathode structure, a moderate voltage is applied across the two conductors. This should result in a current flow through the semiconductor. Upon application of an external accelerating field, some of the electrons should leave the semiconductor and enter the vacuum.

Because of the variety of the materials and configurations of the cathode structures explored in this study, it is difficult to summarize the experiments in a more general form. In the following paragraphs, the various cathodes are therefore described individually in the sequence in which they were prepared.

### Transverse-Field Cathode # 1

For the preparation of the first cathode, gold and silver were used as the two conductors. The gap between the two metals was defined by a thin film of silicon monoxide ( $\text{SiO}$ ) and was bridged by barium oxide ( $\text{BaO}$ ). The structure of the cathode is sketched in Figure 6 a, b. In detail, the preparation was as follows:

A gold film was vapor-deposited onto a clean and degassed glass substrate. The substrate was cleaned by the same method used for cleaning the substrates of field-emission type of cathodes and described earlier in this report. The degassing of the glass substrate was accomplished by means of a small laboratory-made hotplate mounted closely behind the substrate. The gold was evaporated from an alumina-coated tungsten basket at a basket temperature of about  $1265^\circ\text{C}$  and at a bell jar pressure in the low  $10^{-6}$  torr range. The distance between substrate and vapor source was 4". The thickness of the deposited film was monitored by the quartz crystal method and was estimated to be of the order of  $1000\text{ \AA}$  (frequency change: 10 kHz). The duration of the deposition was about 15 minutes.

Following the gold deposition, about one half of the length of the gold strip was masked, and after a brief degassing of the sample, the other

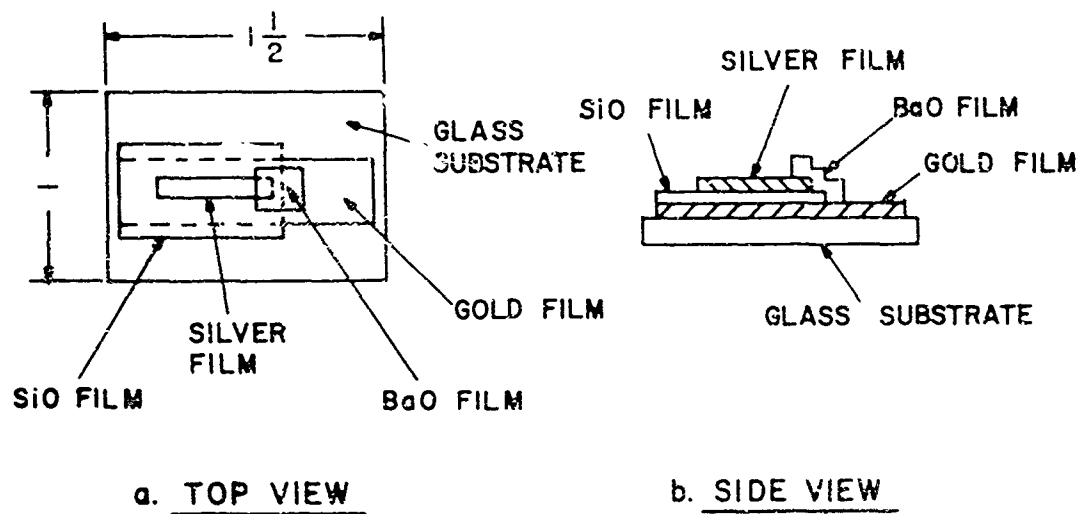


FIGURE 6. STRUCTURE OF TRANSVERSE-FIELD CATHODE <sup>\*</sup>1

half of the strip was coated by a SiO film. An E-gun served as the heat source. Initially, the evaporation of the SiO proceeded quite rapidly (beam current: 40 ma), but soon slowed down considerably as the beam burned out the center of the SiO pellet and reached less and less of the material of the remaining shell. The SiO film was deposited to a thickness of approximately 8000 Å. (Frequency change: 8 kHz; final beam current: 150 ma.)

Using an appropriate mask, a narrow silver strip was deposited onto the SiO film after the sample with the mask had been outgassed. The position of the silver film can be seen from Figure 6 a, b. The silver was evaporated from an alumina-coated tungsten basket at a temperature of about 1050° C. The bell jar pressure was in the lower part of the  $10^{-6}$  torr region. The thickness of the deposited film was 5000 to 6000 Å (frequency change: 30 kHz). The time needed for the deposition was approximately 20 minutes.

The final step in the preparation of the cathode, i.e., the BaO deposition, required an experimental setup that would permit testing of the finished cathode for emission without prior exposure to air since such exposure would harm the BaO coating. Electrical point contacts made from platinum-clad molybdenum wire were therefore applied to the gold and silver strip after the sample had been mounted in the bell jar. A special movable mask was used to confine the BaO deposition to the sample area near the SiO edge that formed the insulating gap between the gold and silver strip. After the active area of the cathode had been produced by depositing BaO over the gap the movable mask could be dropped and a metal plate rotated in front of the active cathode area by means of an external magnet and a coupling plate. The rotary metal plate provided the third electrode for testing the finished cathode for emission into the vacuum and served also as a shield protecting the cathode sample against contamination during the processing of the BaO source. A sketch of the experimental setup is shown in Figure 7.

Barium carbonate ( $\text{BaCO}_3$ ) placed in a platinum-lined alumina-coated tungsten basket was used as the BaO source. The  $\text{BaCO}_3$  was decomposed to BaO in forepump vacuum ( $10^{-3}$  torr; trap filled with liquid nitrogen). The decomposition started at a basket temperature of 1150° C and was completed by gradually raising the temperature of the basket to 1420° C. The bell jar was then pumped to a pressure in the low  $10^{-6}$  torr range. By further increasing the basket temperature to about 1700° C (heater current: 23 A) the BaO evaporation was initiated and the heating continued for a period of 15 to 20 minutes. The resulting BaO film was approximately 500 Å thick (frequency change: 1.2 kHz). The bell jar pressure during the deposition was  $2 \times 10^{-6}$  torr.

The sample was tested in the bell jar using a transistor curve tracer. No current flow between the silver and gold electrode was observed at voltages up to 200 V. The bell jar was removed and the sample inspected. It was found that the gold electrode was damaged by the probe wire and apparently an open circuit had developed. Testing of the sample in air with the probe wires moved to various spots of the electrodes initially showed no current flow either. After several minutes of testing, however, electrical breakdown occurred at all spots tested, probably because of deterioration of the BaO in the moist air.

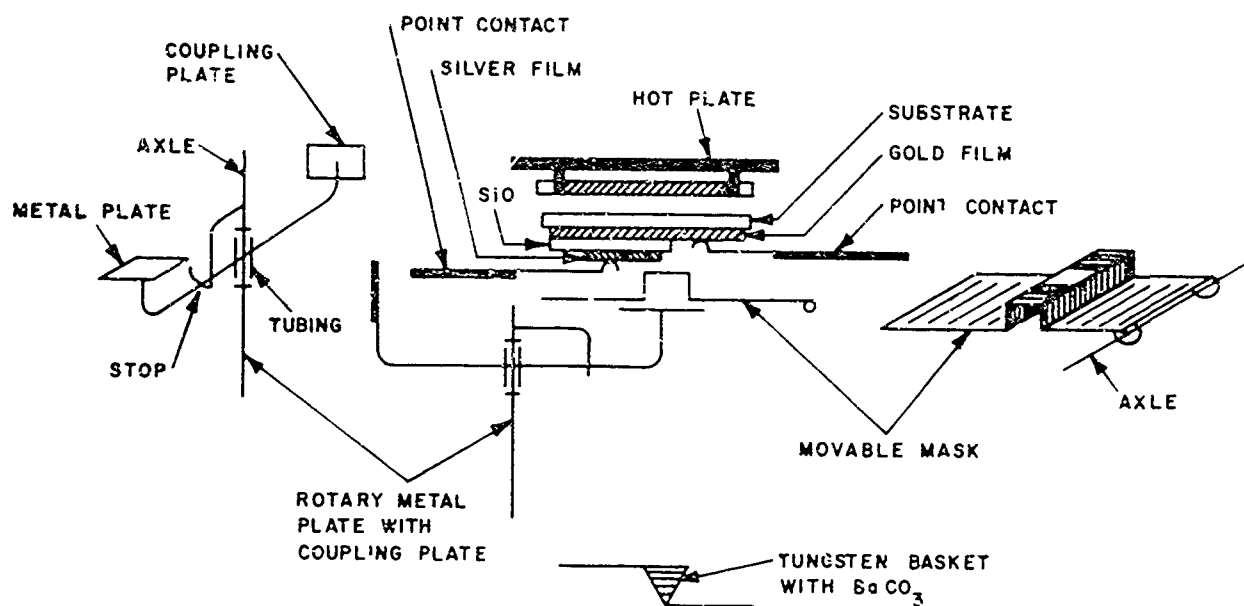


FIGURE 7. TRANSVERSE-FIELD CATHODE #1;  
SETUP FOR BaO DEPOSITION

Since it was assumed that the negative result of the experiment was caused by the failure of the BaO to behave as a semiconductor it was decided to use in future cathode structures nickel as electrode material and to make provision for processing the BaO deposit in a similar way as thermionic BaO cathodes.

#### Transverse-Field Cathodes # 2 through # 5

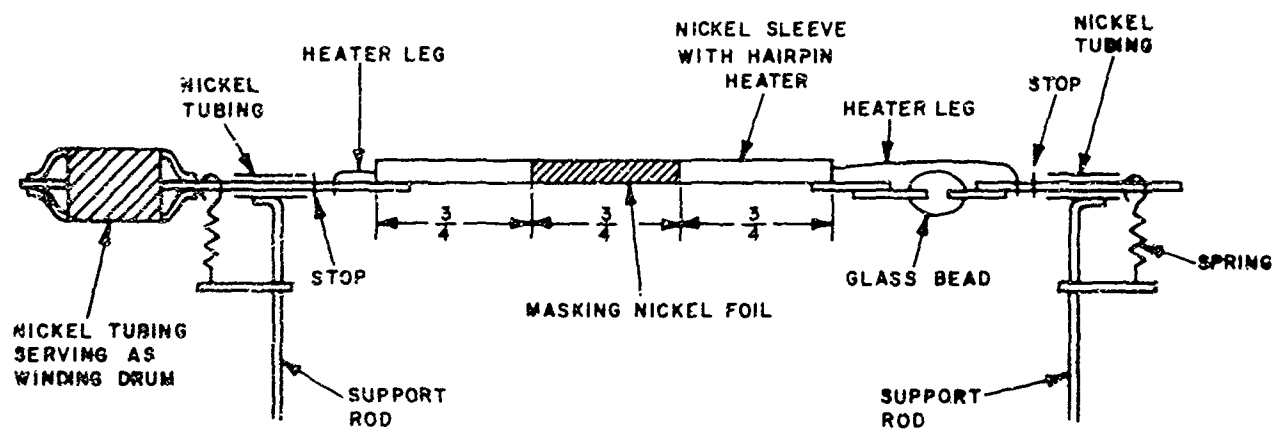
These cathodes have in common that a flat nickel sleeve was used as one of the conductors. The sleeves were furnished with a multiple hair-pin heater for outgassing of the structures and processing of the BaO deposits. The second electrode of all the cathodes was also nickel, but applied in different ways. The gaps between the electrodes were formed by insulating layers (SiO or alumina), or were simply empty space. Unfortunately, with one exception only (Cathode # 5), the gaps of all the various cathode structures proved to be conductive before a BaO film was applied.

The individual cathodes were prepared as follows:

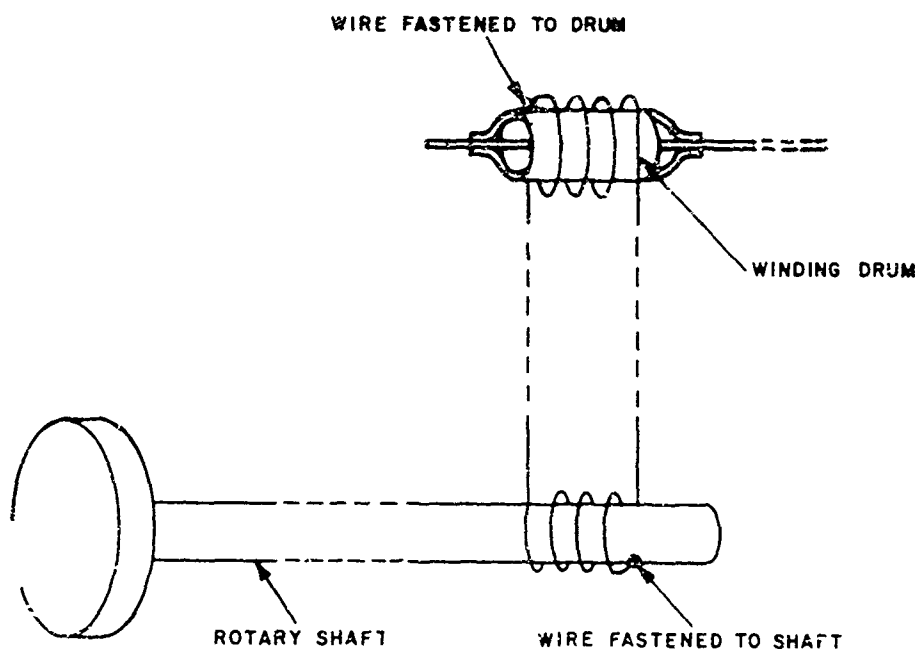
#### Transverse-Field Cathode # 2

A nickel sleeve, about 2 1/4" long, 1/8" wide and 1/16" high, was coated all around by a SiO film with the exception of the middle section of the sleeve that was masked by wrapped-around nickel foil. The necessary rotation of the sleeve during the SiO deposition was carried out manually by means of a rotary shaft introduced into the bell jar through a port of the feedthrough ring. Pieces of nickel rod welded to the ends of the sleeve served as an axle and the motion of the rotary shaft was transmitted to the axle by wire loops. The setup for rotating the sleeve is illustrated in Figure 8.

The SiO was evaporated from an alumina-coated tungsten basket placed at a distance of 5" from the sleeve. Prior to the deposition, the nickel sleeve and the basket with the SiO were degassed simultaneously. The maximum temperature at the ends of the sleeve during the degassing was 1150° to 1175° C. The middle section of the sleeve was 50° to 75° cooler because of the presence of the masking foil. These temperatures were maintained for 25 minutes. The heating of the sleeve was then discontinued. At this time, the temperature of the basket with the SiO was about 1300° C and slow evaporation of the SiO took place. The basket temperature was further raised until the SiO evaporated with sufficient speed to initiate the deposition onto the sleeve by dropping the protective shield placed between basket and sleeve (basket temperature: about 1400° C). The deposition was continued for a period of 30 minutes with the basket temperature finally increased to 1450° C. Because of jamming of the rotary mechanism, the sleeve could be rotated only during the first 15 minutes of the deposition. Fortunately, the jamming occurred when the face of the sleeve onto which nickel strips were later to be deposited to serve as second electrodes was turned toward the SiO source so that this more important side of the sleeve received the heavier coating. From the frequency change of the quartz crystal (1.9 kHz during the rotation of the sleeve, 4.7 kHz with the sleeve stationary), it was estimated that the thickness of the SiO layer on the face of the sleeve was of the order of 5500 Å. The bell jar pressure during the deposition was  $1 \times 10^{-6}$  torr.



#### a. SLEEVE ASSEMBLY



#### b. ROTATING MECHANISM

FIGURE 8. TRANSVERSE-FIELD CATHODE #2: SETUP FOR ROTATING THE NICKEL SLEEVE

After removal of the masking foil, two nickel strips were deposited through an appropriate mask onto the SiO-covered areas of the sleeve in such a way that the strips extended almost to the border between the SiO coatings and the bare area of the nickel sleeve (see Figure 9). Each nickel strip represented a second electrode, while the SiO layer formed the insulating gap between the nickel strips and the bare nickel area of the sleeve. Two potential cathode areas were thus produced on the sleeve.

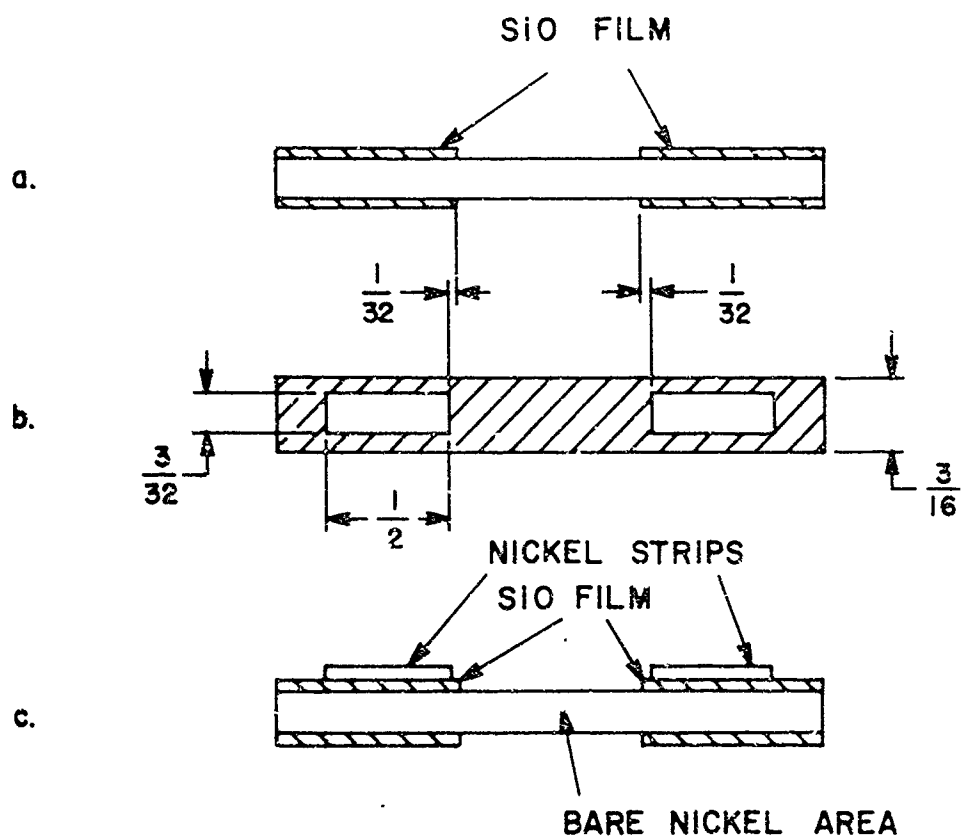
The nickel source consisted of short pieces of 0.05" nickel wire placed in an alumina-coated tungsten basket. Prior to the nickel deposition, the sleeve with the SiO coating was degassed by raising its temperature within 35 minutes to 820° C and maintaining this temperature for 40 minutes. During these 40 minutes, the nickel source was gradually heated to about 1550° C. The nickel slowly evaporated at this temperature. The sleeve was now allowed to cool while the temperature of the basket was further increased to expedite the nickel evaporation. After 20 minutes, the shutter that shielded the sleeve from the nickel source was dropped and the nickel deposited onto the sleeve. The deposition was continued for 15 minutes at a bell jar pressure of  $1.5 \times 10^{-6}$  torr. Since a considerable nickel deposit had formed on the bell jar wall during the outgassing of the nickel source and a pyrometer was used for the temperature measurements it was not possible to determine the temperature of the basket during the deposition of the nickel. Most likely, this temperature was about 1650° C.

The thickness of the nickel layer was somewhat larger than the value indicated by the frequency change of the quartz crystal (10 kHz, corresponding to about 2000 Å) because the crystal was one inch farther away from the nickel source than the sleeve (sleeve-to-source distance: 4"). The pressure in the bell jar was  $1.5 \times 10^{-6}$  torr during the deposition of the nickel.

The sample was removed from the bell jar and tested with a continuity meter for electrical isolation of the nickel strips from the sleeve. A short circuit existed between each of the nickel strips and the sleeve. Since it was clearly visible that the SiO coatings extended far enough beyond the edges of the nickel strips to rule out the possibility of a direct contact between the strips and the bare area of the sleeve the electrical short must have occurred through the bulk of the SiO layer. Application of a heavier SiO coating was therefore tried in the next experiment.

### Transverse-Field Cathode # 3

The structure of this cathode was identical with that of Transverse-Field Cathode # 2, but several changes were made in the experimental procedures. In particular, the setup for rotating the nickel sleeve during the SiO deposition was improved. Instead of the two pieces of nickel rod that served as the axle for the sleeve in the previous setup, one solid nickel rod was used in the present experiment. The mounting of the glass bead that electrically isolated the ends of the multiple hairpin heater (see Figure 8) was also changed. In the new arrangement, the bead was welded to two short pieces of tubing one of which was slipped over one end of the sleeve axle and spot-welded; the other short piece of tubing firmly



- a. NICKEL SLEEVE WITH SiO FILM (SIDE VIEW)
- b. MASK FOR NICKEL DEPOSITION (TOP VIEW)
- c. NICKEL SLEEVE WITH SiO FILM AND NICKEL STRIPS (SIDE VIEW)

FIGURE 9. TRANSVERSE — FIELD CATHODE #2 : DEPOSITION OF THE NICKEL STRIPS

accommodated a piece of nickel rod of the same thickness as the sleeve axle. A straighter and more rigid axle resulted from these changes.

As another modification, the piece of wide nickel tubing that had been attached in the previous setup to the axle of the sleeve to serve as winding drum for the driving wire was replaced by a spool machined from stainless steel. The elevated rims of the spool prevented the driving wire from gliding off. The spool was slipped onto the axle and held in position by a countersunk setscrew. To fasten the driving wire to the spool the wire was threaded through two fine holes bored side-by-side through one of the rims of the spool. A second similar spool was machined with a tubular appendage for attaching the spool to the rotary shaft.

Finally, the support of the axle of the sleeve was modified. The nickel tubings used as bearings in the previous setup were discarded. In the new arrangement, the axle rested in small holes bored through short pieces of stainless steel rod of the type regularly used for assembling experimental setup in the bell jar. The rods, in turn, were attached by standard clamps to the vertical support rods of the bell jar.

It should be also noted that heavier nickel foil was used for masking the middle part of the nickel sleeve and that the foil was not completely wrapped around the sleeve, but covered only the face and the sides. These changes in the masking procedure were made to facilitate the removal of the mask after the SiO deposition. Some difficulties had been experienced in this respect during the preparation of the previous cathode.

The procedure of degassing the nickel sleeve and the tungsten basket with the SiO was very similar to that followed in the preparation of Cathode # 2. The maximum temperature at which the sleeve was outgassed was approximately  $1100^{\circ}\text{C}$ . The sleeve was kept at this temperature for 25 minutes and was then allowed to cool. The degassing of the basket with the SiO was started simultaneously with the outgassing of the sleeve. At the time at which the heater current of the sleeve was turned off the basket temperature was about  $1250^{\circ}\text{C}$ . This temperature was raised within the next 35 minutes to  $1350^{\circ}\text{C}$  and the deposition of the SiO onto the sleeve was initiated. The sleeve-to-SiO source distance was 4" (compared to 5" in the case of Cathode # 2). The deposition of the SiO was carried on over a period of 1 1/4 hour (bell jar pressure:  $1 \times 10^{-6}$  torr). For unknown reasons, the quartz crystal did not function properly so that the thickness of the SiO deposit had to be judged by the changes in interference colors. The finished layer was estimated to be several thousands angstroms thick, but it was difficult to decide whether the produced layer was thicker than the SiO layer of Cathode # 2 as it was originally planned.

The mechanism for rotating the nickel sleeve functioned satisfactorily throughout the entire SiO deposition although slackening of the driving wire presented a problem sometimes.

The deposition of the nickel strips onto the SiO layer was performed through the same mask used in the preparation of Cathode # 2. An alumina-coated tungsten basket filled with short pieces of nickel wire served again as the nickel source (sample-nickel source distance: 4"). The

degassing of the nickel source and the sleeve with the SiO layer followed essentially the method employed in fabricating Cathode # 2. First, the sleeve was heated within 30 minutes to approximately 800° C. Subsequently, the outgassing of the basket with the nickel was started while the degassing of the sleeve continued at about 800° C for 55 minutes. During this period, the basket temperature was raised to approximately 1100° C. The heating of the sleeve was now discontinued. After a period of about one hour, the basket temperature was further increased until (after 15 minutes) the nickel evaporated sufficiently fast to initiate the deposition onto the sleeve by removing the shutter placed as usual between sleeve and nickel source. The nickel deposition was completed within 10 minutes. According to the frequency change of the quartz crystal (20 kHz), the estimated thickness of the nickel layer was approximately 4000 Å. The pressure in the bell jar during the nickel deposition was  $1.4 \times 10^{-6}$  torr. Because of clouding of the bell jar wall during the outgassing of the nickel source, the basket temperature at the time of the nickel deposition could not be measured with reasonable accuracy, but appeared to be considerably lower than the basket temperature during the deposition of the nickel strips of Cathode # 2.

Examination of the sample revealed that, as in Cathode # 2, the nickel strips were far enough away from the critical edge of the SiO layer to eliminate the possibility of a direct contact with the bare area of the nickel sleeve. But, nevertheless, testing with the continuity meter indicated, as in Cathode # 2, an electrical short between each nickel strip and the nickel sleeve. Using probe wires and the transistor curve tracer, electrical shorts were also observed across the SiO surface along the sides of the sleeve at voltages as low as 1 volt although occasionally spots were found where the voltage could be raised to several volts (up to 35 V) before breakdown occurred. Microscopic inspection (150X) showed no obviously faulty spots in the SiO or nickel coatings, but revealed a considerable roughness of the surface which evidently resulted from the rough surface of the nickel sleeve. There were two possible explanations for the electrical conductivity of the SiO layer: (1) The roughness of the sleeve may have caused the development of minute cracks in the SiO through which the nickel penetrated during the deposition thereby forming conductive paths; (2) Diffusion of nickel into the otherwise sound SiO layer may have occurred during the bake-out of the coated sleeve resulting in degradation of the insulating quality of the SiO.

#### Transverse-Field Cathode # 4

A drastic change was made in the preparation of this cathode inasmuch as aluminum oxide ( $\text{Al}_2\text{O}_3$ ) was chosen as the insulator for forming the gaps between the conductors, and a spraying technique was used for applying the  $\text{Al}_2\text{O}_3$  to the nickel sleeve. As in the preparation of Cathodes # 2 and # 3, the middle section of the sleeve was masked by a strip of nickel foil before the sleeve was coated all around by  $\text{Al}_2\text{O}_3$  (commercial  $\text{Al}_2\text{O}_3$  suspension, diluted by an equal volume of amyl acetate; ten spray gun passes). The thickness of the  $\text{Al}_2\text{O}_3$  coating was several microns. The sleeve with the coating was fired in hydrogen at about 1300° C.

Another feature distinguishing Cathode # 4 from Cathodes # 2 and # 3 was that two additional gaps were produced that differed from the

type of gaps used in the earlier cathodes. In Cathodes # 2 and # 3, two identical gaps were formed between the bare area of the nickel sleeve and each one of the nickel strips deposited on the top of the insulating layer (see Figure 9). Two gaps of this type were also present in Cathode # 4, but in addition, gaps were produced in the nickel strips, one each in each strip, by simply using thin wires as masks while depositing the strips. To provide electrical contact to the various sections of the nickel strips, ribbons of nickel foil were wrapped around the  $\text{Al}_2\text{O}_3$ -coated sleeve before the nickel strips were deposited. To prevent short-circuiting of the  $\text{Al}_2\text{O}_3$  coating at the ends of the sleeve by nickel creeping around the edges during the deposition, masking strips of nickel foil were attached to the ends of the sleeve. A side view of the  $\text{Al}_2\text{O}_3$ -coated sleeve with the masking wires, the contact ribbons and the masking strips attached is shown in Figure 10.

In contrast to the procedure followed in the preparation of Cathodes # 2 and # 3, the nickel foil wrapped around the middle section of the sleeve prior to the spray-coating with  $\text{Al}_2\text{O}_3$  was not removed before the nickel strips were deposited onto the  $\text{Al}_2\text{O}_3$ . It was therefore not necessary to use the more elaborate mask required for the nickel deposition when preparing Cathodes # 2 and # 3. Instead, a simple nickel frame was applied to the sample as mask merely for the purpose of restricting the nickel deposition to the face of the sleeve. The degassing of the sleeve and the nickel source was performed under conditions similar to those described for Cathodes # 2 and # 3. The nickel was deposited within 10 minutes to a thickness of about 3000 Å at a bell jar pressure of  $2 \times 10^{-6}$  torr. After removal of the various masks, a structure was obtained as shown in Figure 11. Included in the figure are the circuits used for testing the gaps.

When the gaps were electrically tested a short circuit was found to exist between each section of the nickel strips and the nickel sleeve, i.e., all the gaps were by-passed. It was furthermore observed that the contact ribbons had loosened. In addition, the adherence of the nickel deposit to the  $\text{Al}_2\text{O}_3$  coating was poor. It should be also noted that the removal of the various masks had caused difficulties because the masks were fused more or less solidly to the sleeve. The nickel foil mask underneath the  $\text{Al}_2\text{O}_3$  in the center part of the sleeve was especially hard to remove because it was bound very tightly to the sleeve probably due to the high temperature of the hydrogen-firing of the sleeve after the  $\text{Al}_2\text{O}_3$  deposition.

#### Transverse-Field Cathode # 5

Since there was the possibility that nickel had penetrated through the  $\text{Al}_2\text{O}_3$  coating during the vapor deposition and had caused the short circuits observed on Cathode # 4 it was decided to use strips of nickel foil as second electrodes for the preparation of Cathode # 5.

As the first step in preparing the cathode, a nickel sleeve was mounted on a nickel rod and furnished with masks of nickel foil as shown in Figure 12. The sleeve was then spray-coated with  $\text{Al}_2\text{O}_3$  and, after removal of the masking strips, fired in hydrogen. (The masking strips were removed prior to the hydrogen firing to eliminate the difficulty experienced in the preparation of Cathode # 4 from the fusing of the masking strips to the sleeve.) Subsequently, the partially  $\text{Al}_2\text{O}_3$ -coated sleeve was provided

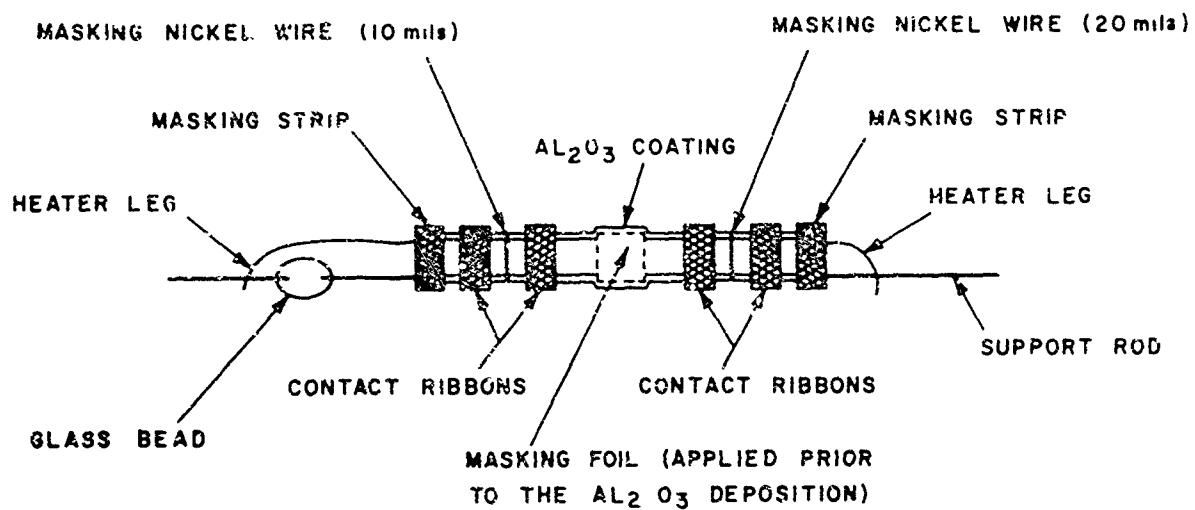


FIGURE 10. TRANSVERSE-FIELD CATHODE #4 : AL<sub>2</sub>O<sub>3</sub> - COATED SLEEVE READY FOR THE DEPOSITION OF THE NICKEL STRIPS (SIDE VIEW)

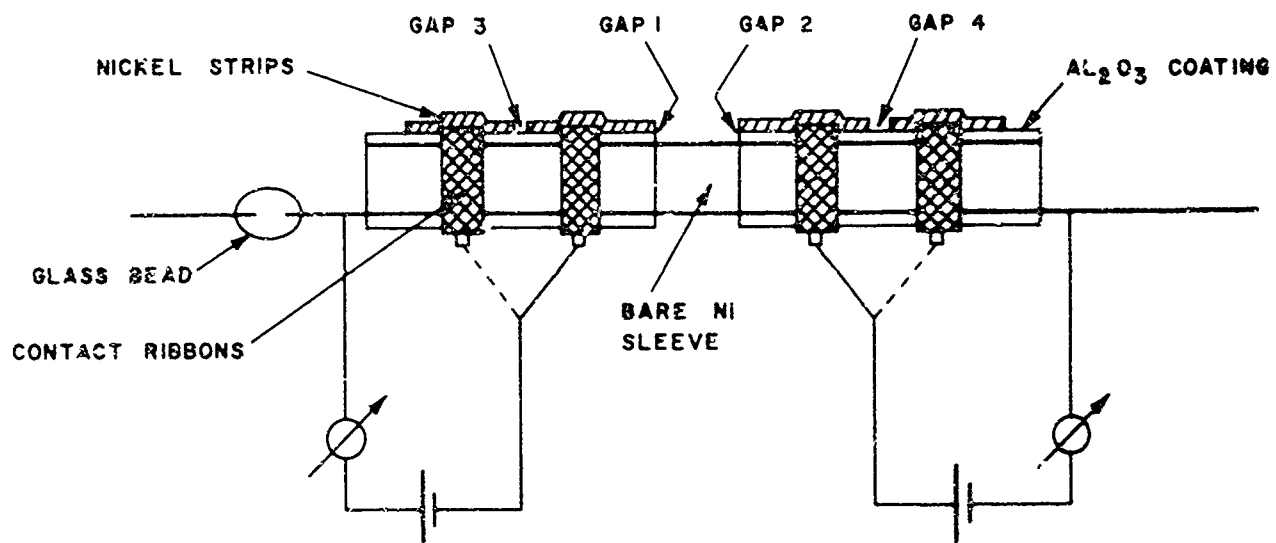


FIGURE II TRANSVERSE-FIELD CATHODE #4: SIDE VIEW OF THE CATHODE AFTER NICKEL DEPOSITION AND REMOVAL OF THE MASKS (TEST CIRCUITS ARE INCLUDED)

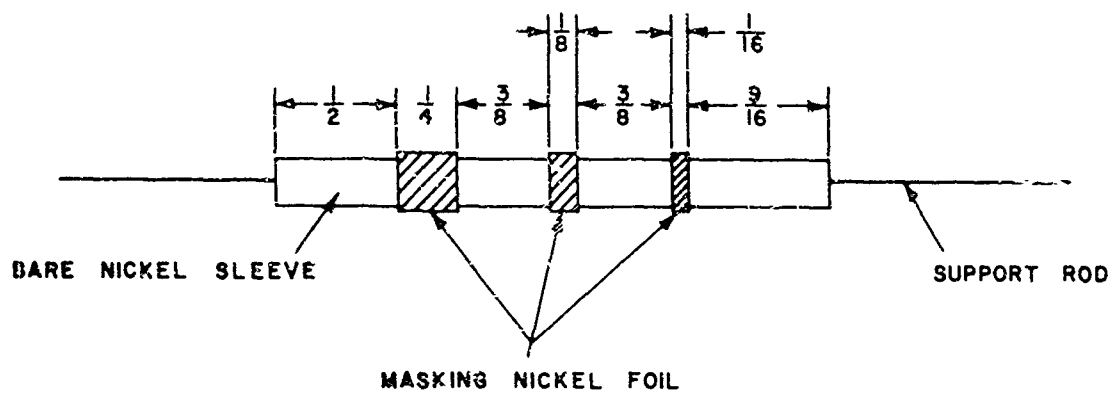


FIGURE 12 FIRST VERSION OF TRANSVERSE-FIELD CATHODE #5:  
NICKEL SLEEVE WITH NICKEL MASKS (TOP VIEW)

with six strips of nickel foil to serve as second electrodes. Each strip was 1/8" wide and was made from nickel foil prefired to soften the foil for easier and safer mounting of the strips. The strips were wrapped around the  $\text{Al}_2\text{O}_3$ -coated section of the sleeve in close vicinity to the bare nickel areas and fastened by twisting short pieces of thin nickel wires welded to the ends of each strip (see Figure 13). Testing of the nickel strips for electrical isolation from the sleeve revealed, however, that a short circuit existed between each nickel strip and the sleeve. The explanation of this failure was that the twisted wires had cut through the  $\text{Al}_2\text{O}_3$  during the fastening of the strips and had come in direct contact with the support rod of the sleeve. To eliminate this problem the method of mounting the sleeve was changed as indicated in Figure 14. Instead of attaching the sleeve directly to the support rod the sleeve was fastened by nickel straps to a ceramic tubing and the tubing with the sleeve was slipped over the support rod. To keep the sleeve in a fixed position and to simultaneously provide electrical contact between the sleeve and the support rod short pieces of nickel wire were welded across the mounting straps at the ends of the sleeve and the support rod.

A nickel sleeve was mounted to the support rod by the modified method and a structure prepared following the same procedures used in the preparation of the first version of Cathode # 5 (see Figure 13). After electrical tests at voltages up to 200 V had demonstrated that no electrical short existed between any of the nickel contact strips and the sleeve the structure was spray-coated with triple-carbonate (20 spray gun passes to the face and each side of the structure using a triple-carbonate suspension of 40 volume parts commercial suspension and 60 volume parts amyl acetate). Subsequently, the sleeve was furnished with a multiple hairpin heater to permit processing of the triple-carbonate. Pieces of thin nickel wire were welded to the twisted wires of the contact strips for making the necessary electrical connections. Finally, the structure was mounted together with a collector electrode and a sliding mask for protection of the collector during the processing of the triple-carbonate. Figure 15 shows a schematic of the setup including the electrical connections to the terminal board of the pump-station. A test of the structure for leakage currents at voltages up to 200 V was negative.

To process the triple-carbonate the sleeve was gradually raised within 1 hour and 45 minutes to a maximum temperature of  $1280^\circ\text{C}$  measured in the middle section of the sleeve. The temperature of the contact strips was considerably lower ranging from about  $1050^\circ\text{C}$  (measured at a contact strip near the middle of the sleeve) to about  $950^\circ\text{C}$  (measured at the contact strip nearest to the upper end of the sleeve). Immediately upon reaching the maximum temperature, the heater current was reduced and the sleeve maintained at a temperature of about  $900^\circ\text{C}$  for 15 minutes. The pressure in the bell jar rose from  $1 \times 10^{-6}$  torr at the beginning of the processing of the triple-carbonate to a maximum of  $1 \times 10^{-5}$  torr, had declined to  $3 \times 10^{-6}$  torr at the maximum sleeve temperature and was  $1 \times 10^{-6}$  torr during the final heating of the sleeve at  $900^\circ\text{C}$ .

Unfortunately, the support rod of the sleeve warped during the heating and the lower end of the sleeve was pressed against the sliding mask. The mask did therefore not drop when the thin wire holding it in

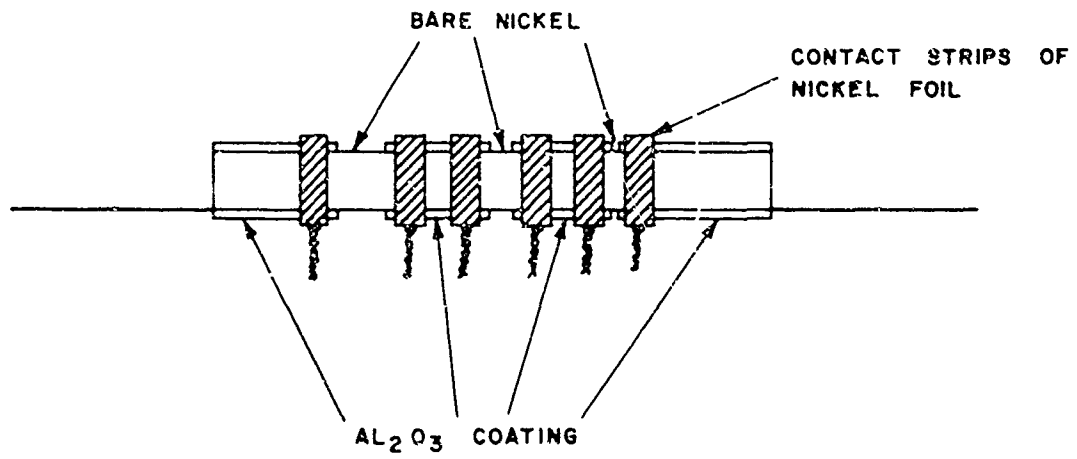


FIGURE 13 FIRST VERSION OF TRANSVERSE-FIELD CATHODE # 5:  
NICKEL SLEEVE PARTIALLY COATED WITH  $Al_2O_3$   
AND FURNISHED WITH CONTACT STRIPS (SIDE VIEW)

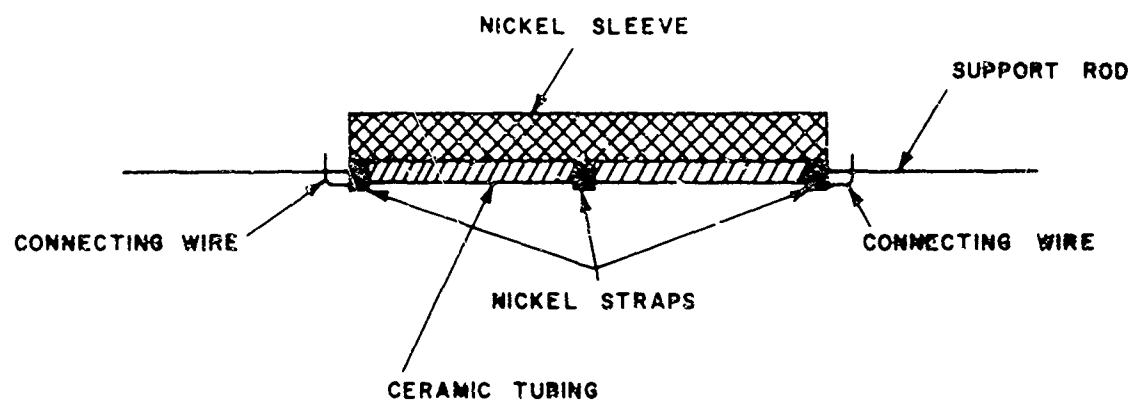
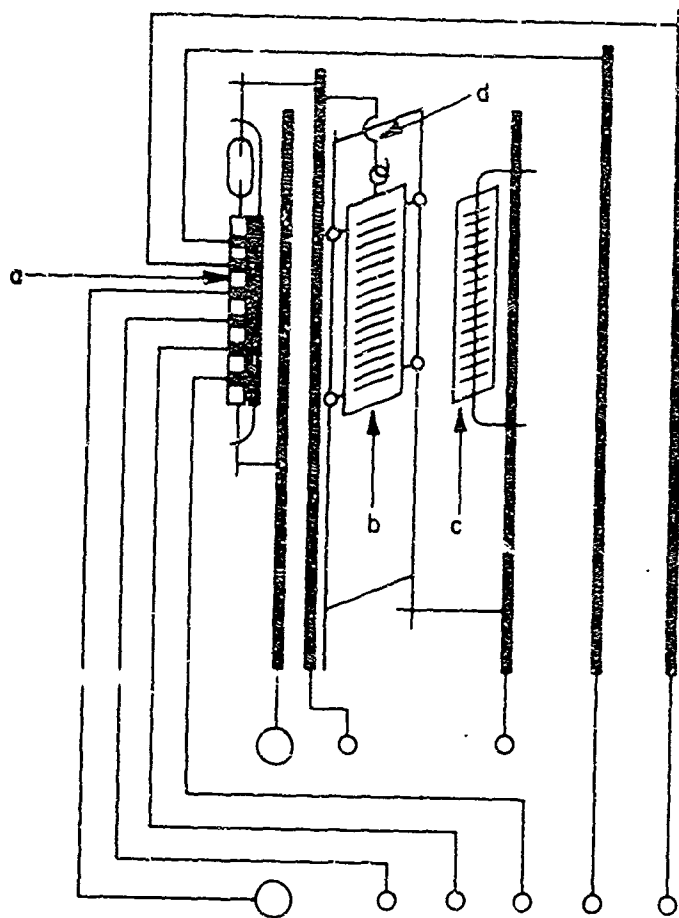


FIGURE 14 FINAL VERSION OF TRANSVERSE-FIELD CATHODE #5:  
IMPROVED METHOD OF MOUNTING THE SLEEVE



- a : SLEEVE WITH CONTACTS
- b : SLIDING SHIELD
- c : COLLECTOR ELECTRODE
- d : BURN-OUT WIPE  
(FOR DROPPING THE SHIELD)

FOR BETTER CLARITY, THE  
DISTANCES BETWEEN SLEEVE,  
SHIELD AND COLLECTOR ELECTRODE  
ARE GREATLY EXAGGERATED  
IN THE SCHEMATIC.

FIGURE 15. FINAL VERSION OF TRANSVERSE-FIELD CATHODE #5:  
SETUP FOR FINAL PROCESSING AND TESTING

position was burnt after completion of the processing. In addition, the impact of the sleeve on the mask had electrically shorted the two elements. It was therefore impossible to test the sleeve for thermionic emission and, hence, to determine whether a sufficiently active BaO had been produced. The short circuit between sleeve and mask also eliminated the possibility of testing the structure for cold cathode emission. Only tests for current flow through the BaO could be performed.

It was found that no current passed between the sleeve and four of the contact strips when tested with a transistor curve tracer at voltages up to about 200 V in either direction. Immediate electrical breakdown occurred at the remaining two contact strips. The bell jar was exposed to air and the structure removed. Inspection revealed some holes burnt into the sleeve indicating partial overheating of the sleeve during the processing of the BaO. As observed on Cathode # 4, it was furthermore found that the contact strips had loosened and were not in satisfactory contact any more with the  $\text{Al}_2\text{O}_3$  coating. This might explain the open circuits between the sleeve and most of the contact strips whereas the observed electrical breakdowns probably originated from mechanical damage of the  $\text{Al}_2\text{O}_3$  coating.

From the poor results of the experiment it was concluded that the simple method of using spray-coatings as insulating layers and metal strips as second electrodes was too crude to produce reliable devices and it was therefore decided to use vacuum techniques again for the preparation of future cathode structures.

#### Transverse-Field Cathode # 6

Basically, this cathode consisted of a nickel strip with a light magnesium undercoating deposited onto a sapphire substrate. The nickel strip was divided into three sections by two gaps. The gaps were bridged by a BaO film. The configuration of the cathode is shown in Figure 16 a, b.

The sapphire substrate was identical in size with the sapphire substrates used in the experiments with the field-emission type of cathodes. The same furnace as in these experiments was therefore employed for the initial degassing of the substrate and the subsequent heat treatments of the sample. To produce the gaps in the nickel strip and the magnesium undercoat the substrate was covered by a mask consisting of a rectangular nickel frame with two wires spot-welded in a direction parallel to the smaller sides of the frame. The thickness of the wires was 20 and 40 mils respectively. The magnesium source was an alumina-coated tungsten basket charged with small packages of folded magnesium ribbon. Short pieces of nickel wire placed in another alumina-coated tungsten basket served as the nickel source. The substrate-to-magnesium source distance was  $4 \frac{3}{4}$ ". The distance between nickel source and substrate was 5".

The substrate with the mask, the magnesium source and the nickel source were degassed simultaneously. The substrate was degassed at  $1200^\circ \text{C}$ , the nickel source at  $1100^\circ - 1150^\circ \text{C}$ . The magnesium source was heated to a faint red-glow. The substrate and the nickel source were then allowed to cool while the heating of the magnesium source was continued until a deposit of approximately 400 Å thickness had formed on the substrate (frequency change of the monitoring quartz crystal: 0.4 kHz). The magnesium

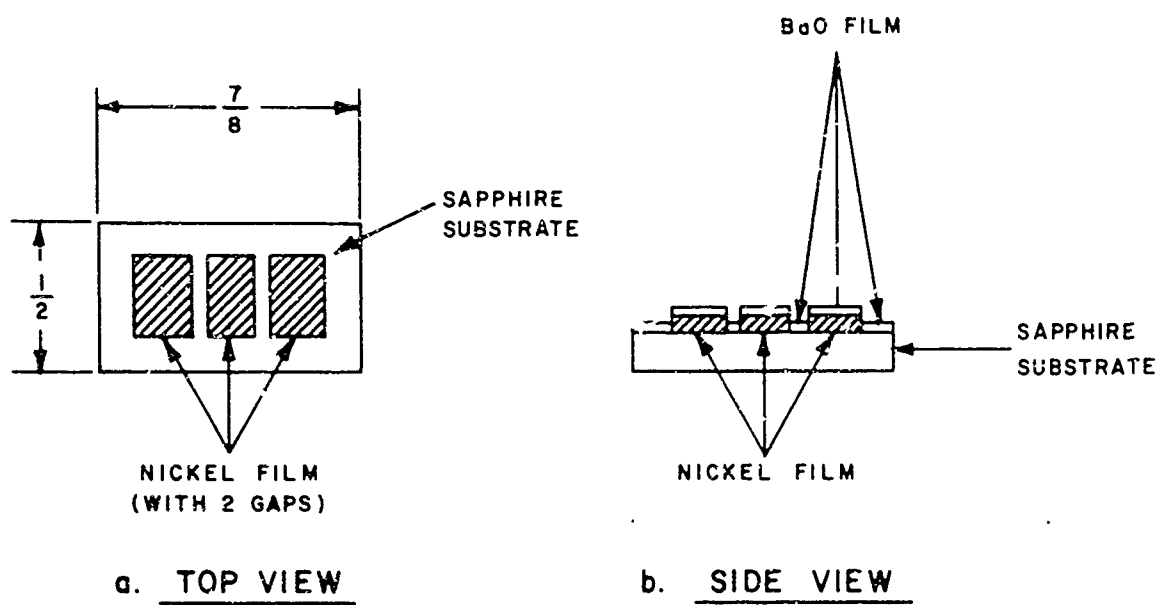


FIGURE 16. STRUCTURE OF TRANSVERSE-FIELD CATHODE #6

undercoating was applied to serve later as a reducing agent for the BaO.

Immediately following the magnesium deposition, the nickel was evaporated onto the substrate by heating the nickel source within 30 minutes to  $1450^{\circ}\text{C}$  and maintaining a temperature of  $1450^{\circ}$  to  $1500^{\circ}$  for another 10 minutes. The estimated thickness of the nickel deposit was 5000 to 6000 Å (frequency change of the quartz crystal: 28 kHz). The nickel layer was finally aged by heating the sample at approximately  $1100^{\circ}\text{C}$  for a period of about 20 minutes.

Prior to bridging the gaps in the nickel layer by the BaO film, a suitable setup had to be devised that would permit electrical testing of the finished cathode structure without intermediate exposure to air. A similar arrangement was used as in the final step of the preparation of Cathode # 1 where the same problem had existed. Several improvements of the earlier setup were made. Instead of one point contact, two electrically independent contacts were applied to each section of the nickel layer. Besides thereby doubling the chance of maintaining electrical contact to each nickel area, this arrangement also provided a possibility of proving that a nickel area was definitely electrically contacted. Electrical continuity between the two point contacts of the nickel area provided this proof.

As another improvement of the setup, the point contacts were applied to the three sections of the nickel layer in such a way that the set of six contacts and the furnace with the cathode sample formed a single, compact unit that could be assembled outside the bell jar. This facilitated the delicate adjustment of the point contacts and resulted also in a sturdier structure. To further simplify the setup the BaO deposition was not restricted to the gap areas. The entire cathode sample was rather exposed to the BaO vapors. This procedure eliminated the need for a special mask. A simple shutter protected the sample during the processing of the BaO source. The rotary metal plate used in the preparation of Cathode # 1 was also employed in the present setup to serve as collector electrode.

The BaO source was  $\text{BaCO}_3$  placed in a platinum-lined, alumina-coated tungsten basket. The distance between the sample and the tungsten basket was 4". After degassing the sample and the BaO source, the  $\text{BaCO}_3$  was slowly decomposed in forepump vacuum at temperatures similar to those quoted in the description of Cathode # 1. The pressure was then lowered to the  $10^{-6}$  torr range and the BaO evaporation initiated by raising the BaO source to a temperature of about  $1700^{\circ}$ . The BaO was deposited to a thickness of about 2000 Å (frequency change of the quartz crystal: 4 kHz). The time required for the deposition was 2 1/2 hours. The final temperature of the tungsten basket was  $1730^{\circ}$ . The bell jar pressure was about  $1 \times 10^{-6}$  torr. After completion of the BaO deposition, each pair of point contacts was checked for electrical continuity. All points were found to be in good contact with the nickel areas.

To activate the BaO deposit the bell jar was pumped to a pressure of  $2 \times 10^{-7}$  torr and the furnace with the sample gradually heated within about 1 hour to  $800^{\circ}\text{C}$ . A test of the nickel area in the middle of the sample for thermionic emission showed a current of about 1 microamp with 100 V applied to the rotary collector electrode. Raising of the temperature

resulted in increased currents but slumping of the emission, probably due to poisoning, was observed at each current increase. At 985° C, for instance, an initial current of 11.5 microamps was obtained gradually decreasing to about 4 microamps within 10 minutes. Approximately the same emission was measured when testing the other two nickel areas of the sample. The pressure during these tests was about  $7 \times 10^{-7}$  torr. The heating was continued at a furnace temperature of about 1000° C for five hours while various emission measurements were made. No particular improvement of the thermionic emission was observed. With the furnace still operating, the sample was finally tested for current flow across the gaps using a transistor curve tracer. With a maximum voltage of 10 V applied across the gaps, the maximum current readings were as follows:

Across the 20 mils wide gap:	50 mA
Across the 40 mils wide gap:	35 mA
Across the two gaps in series:	20 mA.

After discontinuing the heating and allowing the furnace to cool for 20 minutes, the measurements were repeated with the following results:

Current across the 20 mils wide gap:	30 mA
Current across the 40 mils wide gap:	20 mA
Current across both gaps in series:	12 mA.

Repetition of the measurements after leaving the sample in the valved-off bell jar over night and then re-pumping the bell jar to  $1 \times 10^{-7}$  torr resulted in the following current values:

Across the 20 mils wide gap:	27 mA
Across the 40 mils wide gap:	19 mA
Across the two gaps in series:	11 mA.

In all three sets of measurements, the data were independent of polarity (as to be expected) and the VI-characteristics were strictly ohmic.

Testing of the sample for cold cathode emission was attempted by applying a constant voltage of 15 V across the 20 mils wide gap (gap current: 42 mA) and raising the rotary collector electrode to a maximum voltage of 500 V. No emission was observed. The failure of the test was not surprising considering the relatively large width of the gap. With the gap being 20 mils wide and at a bias voltage of 15 V, an electric field of only 300 V/cm existed across the gap. This field strength was much too low to generate electrons with sufficient energy to escape into the vacuum. A direct experimental proof that such energetic electrons were indeed missing in the present experiment was the ohmic nature of the VI-characteristics of the gap currents.

To create electrons capable of entering the vacuum electric fields of the order of  $10^6$  V/cm would be required. Using moderate bias voltages the gaps of future cathode structures should be therefore only a fraction of a micron wide. The use of a simple masking wire for producing such narrow gaps was considered as inadequate. In the following experiments, the width of the gaps was therefore controlled by a vapor-deposited insulating film sandwiched between the conductors.

#### Transverse-Field Cathodes # 7 and # 8

Cathodes # 7 and # 8 were identical in structure. Nickel was used as electrode material. The gap-forming insulator was SiO. The sapphire substrate had the same dimensions as that used for the preparation of Cathode # 6. A sketch of the configuration of Cathodes # 7 and # 8 is shown in Figure 17 a, b. The preparation procedures were as follows:

#### Transverse-Field Cathode # 7

As usual, an alumina-coated tungsten basket filled with pieces of nickel wire served as the nickel source. The distance between substrate and nickel source was 4". The furnace with the substrate and the nickel source were degassed simultaneously. The furnace was heated to 1230° C within 35 minutes and then allowed to cool while the temperature of the nickel source (1265° C) was further raised until, after 15 minutes, the nickel evaporated with sufficient speed to initiate the deposition onto the substrate by removing the shutter located between nickel source and substrate (nickel source temperature: 1400° to 1500° C). The nickel deposition was completed within 10 minutes. The thickness of the deposit was 6000 to 7000 Å (frequency change of the quartz crystal: 30 kHz). The bell jar pressure during the deposition was  $1 \times 10^{-6}$  torr. Subsequently, the nickel layer was aged by heating at 1000° C for a period of 15 minutes.

The SiO was evaporated from an alumina-coated tungsten basket placed at a distance of 4" from the sample. The SiO deposition was preceded by a bakeout of the sample and the SiO source. Both were heated simultaneously. The temperature of the furnace with the sample was raised within 40 minutes to 1215° C. The temperature of the SiO source was at that time 1030° C. The heating of the sample was then discontinued and the temperature of the SiO source further increased within 30 minutes to 1400° C. The protective shield between sample and SiO source was dropped and the SiO deposition initiated. The SiO was deposited over a period of 80 minutes with the temperature finally raised to 1460° C (bell jar pressure: low  $10^{-7}$  torr region). The estimated thickness of the layer was approximately 5000 Å (frequency change: 5 kHz).

The top nickel film was deposited under similar conditions as the nickel base layer with the exception that the bakeout of the sample prior to the nickel deposition and the final aging of the top nickel film were performed at a maximum temperature of 900° C. (The corresponding temperatures during the preparation of the nickel base layer were 1230° C and 1000° C respectively.) The thickness of the top nickel film was 5000 to 6000 Å.

Testing of the sample for electrical isolation of the two nickel layers indicated a short circuit. Since microscopic examination of the sample clearly showed that the critical edge of the top nickel film did not extend beyond the SiO layer the short circuit could be obviously explained only by electrical conductivity of the SiO layer. However, when point contacts were applied to the bare SiO surface near the top nickel film in the region where this film and the nickel base layer were superimposed no short circuits were detected between the SiO surface and either the nickel base layer or the top nickel film. It seemed, therefore, that the SiO layer

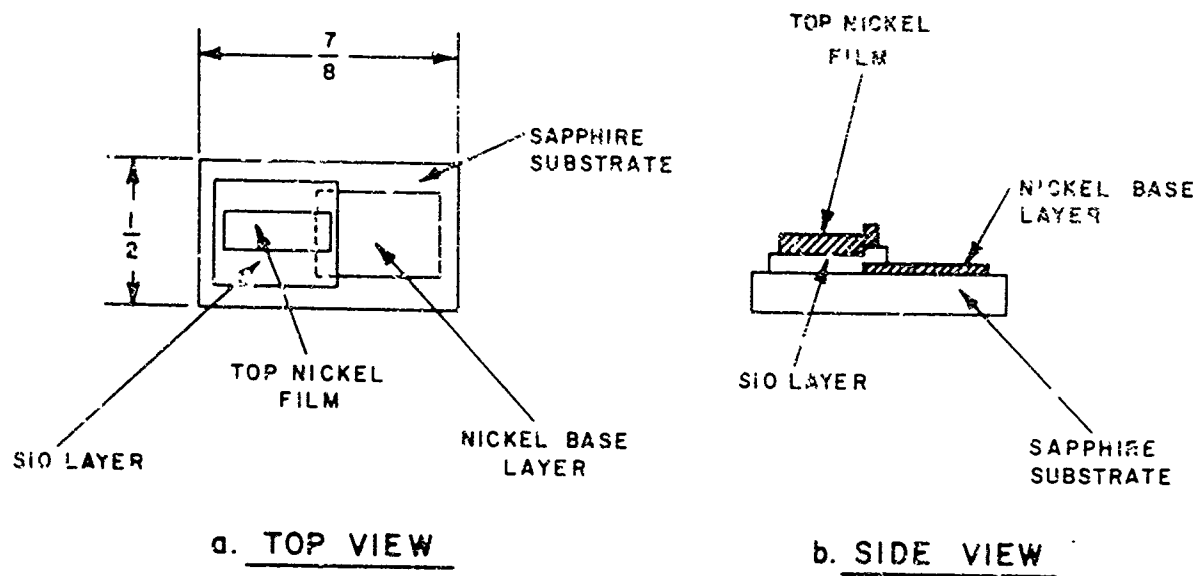


FIGURE 17.  
STRUCTURE OF TRANSVERSE-FIELD CATHODES #7 AND #8  
(SHOWN WITHOUT BaO COATING)

was strongly conductive only where the two nickel layers faced each other. Since the sample had been heated to 900° C before and after the deposition of the top nickel film there was the possibility that nickel had diffused into the SiO increasing its conductivity especially in the region between the two nickel layers because in this region the diffusion took place from two sources. Cathode # 8 was therefore prepared in an attempt to check into this possibility.

#### Transverse-Field Cathode # 8

The deposition of the nickel base layer and the SiO layer followed closely the procedures used in the preparation of Cathode # 7. However, to reduce the possibility of nickel diffusion into the SiO to a minimum the bakeout of the sample prior to the deposition of the top nickel film was performed at a moderate temperature (about 500° C as compared to 900° C in the case of Cathode # 7) and the final aging of the top nickel film was abandoned completely.

In spite of these precautions, a short circuit existed again between top nickel film and nickel base layer. The assumption that nickel diffusion had caused the failure of Cathode # 7 appeared therefore to be erroneous. As the simplest alternate explanation for the existence of the short circuit there remained the possibility that the top nickel strip was in direct contact with the edge of the nickel base layer inside the cathode structure due to insufficient thickness of the SiO layer. Figure 18 illustrates the situation. To eliminate this possible source of failure in future experiments the SiO layer should be made thicker than the nickel base layer, or the SiO deposition should be performed at an angle.

#### Transverse-Field Cathodes # 9 through # 11

For a special application, a transverse-field cathode was required that differed in its configuration from the cathodes explored thus far. Basically, the new cathode structure consisted of a cylindrical metal pellet with one flat surface covered by an insulating layer with a hole in its center. The bare metal area exposed through the hole served as one electrode. The other electrode was formed by a metal film located on the top of the insulating layer. The insulating layer established the gap between the two electrodes. Bridging of the gap by a BaO film completed the cathode structure. A sketch of the cathode structure is shown in Figure 19. Several attempts were made to produce this type of transverse-field cathode.

As a common practice in the experiments, a molybdenum pellet, 1/4" in diameter and 1/3" high, was used as the base of the structure. The flat surface of the pellet onto which the insulating layer and the top metal film were to be deposited was mechanically polished. To maintain a bare metal area in the center of this surface during the deposition of the insulating layer and the top metal film a short piece of a nickel wire serving as mask was tightly fitted into a shallow hole drilled into the surface. After the deposition of the insulating layer and the top metal film, the nickel wire was removed by etching.

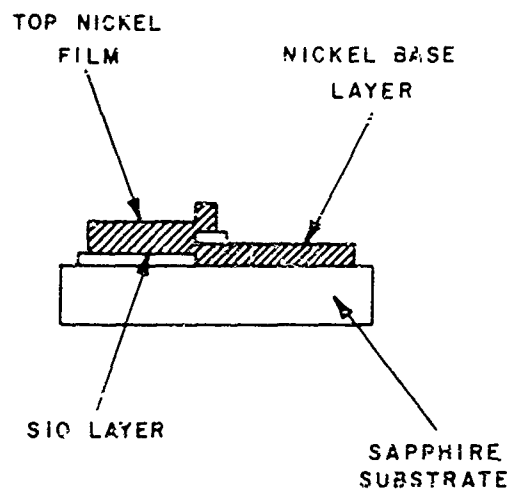


FIGURE 18.

CATHODE STRUCTURE OF THE TYPE OF TRANSVERSE-FIELD  
CATHODES #7 AND #8 WITH ELECTRICALLY SHORTED CONDUCTORS.

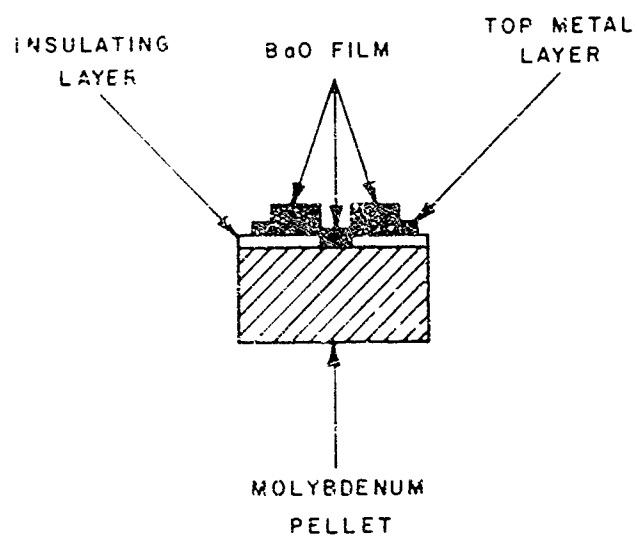


FIGURE 19. BASIC STRUCTURE OF TRANSVERSE - FIELD CATHODES #9 THROUGH #11

Heating of the pellet was accomplished by electron bombardment. Initially, a triple-carbonate-coated coil of tungsten wire surrounding the pellet was used as electron source, but the heating of the coil caused serious sagging of the wires. To overcome this problem the coil was replaced by a single loop, first made from tantalum, finally from tungsten ribbon. The ribbon was 3 mils thick and about 3/32" wide. The diameter of the loop was about 1/2".

Difficulties were also encountered from peeling of the triple-carbonate coating. A very light spray coat (one spray-gun pass) was found to reduce the danger of peeling to a minimum and yet to provide sufficient electron emission.

Several methods of activating the triple-carbonate and heating the molybdenum pellet were tried. The procedure that proved to be most satisfactory was one in which the coated ribbon was gradually raised in forepump vacuum (about  $10^{-3}$  torr) to a temperature between  $1100^{\circ}$  and  $1200^{\circ}$  C to break down the triple-carbonate and to degas the ribbon to a reasonable degree. Subsequently, the bell jar pressure was reduced to the lower  $10^{-6}$  torr region and the ribbon temperature lowered to about  $1000^{\circ}$  C. By applying a positive voltage to the pellet the bombardment of the pellet was initiated starting with a bombarding current of 20 to 30 mA (required pellet voltage: 100 to 200 V). By further raising the pellet voltage the bombarding current was gradually increased until the desired temperature of the pellet was obtained.

The top metal film was deposited onto the insulating film through a mask consisting of a fairly heavy tantalum sheet with a hole somewhat smaller in diameter than the pellet to prevent the metal vapors from creeping around the outer edge of the insulating film and causing an electrical short between the top metal film and the bulk of the pellet. The mask was not in direct contact with the insulating film to avoid damage of the film by scratching. The method of mounting the mask as close as possible to the pellet without touching its surface is illustrated in Figure 20. Mask and pellet formed a single unit that could be easily assembled outside the bell jar. By sliding the nickel wire supporting the pellet into the narrow tubing attached to the mask the distance between mask and pellet could be adjusted safely and accurately. After the adjustment, the nickel wire was firmly attached to the tubing by a spot-weld.

The details of the preparation of Cathodes # 9 through # 11 were as follows:

#### Transverse-Field Cathode # 9

SiO was selected as the insulator and molybdenum as the top metal. The masking nickel wire was 20 mils in diameter. Prior to the deposition of the SiO layer, the molybdenum pellet was degassed for 25 minutes at about  $1000^{\circ}$  C (heat-up time: 30 minutes). The SiO was evaporated from an alumina-coated tungsten basket. The distance between SiO source and molybdenum pellet was 4 1/4". The temperature of the basket was raised within 1 hour and 25 minutes to  $1310^{\circ}$  C. At this temperature, the SiO began to slowly evaporate. The shutter between the SiO source and the molybdenum pellet was then dropped and the SiO deposited onto the pellet with no

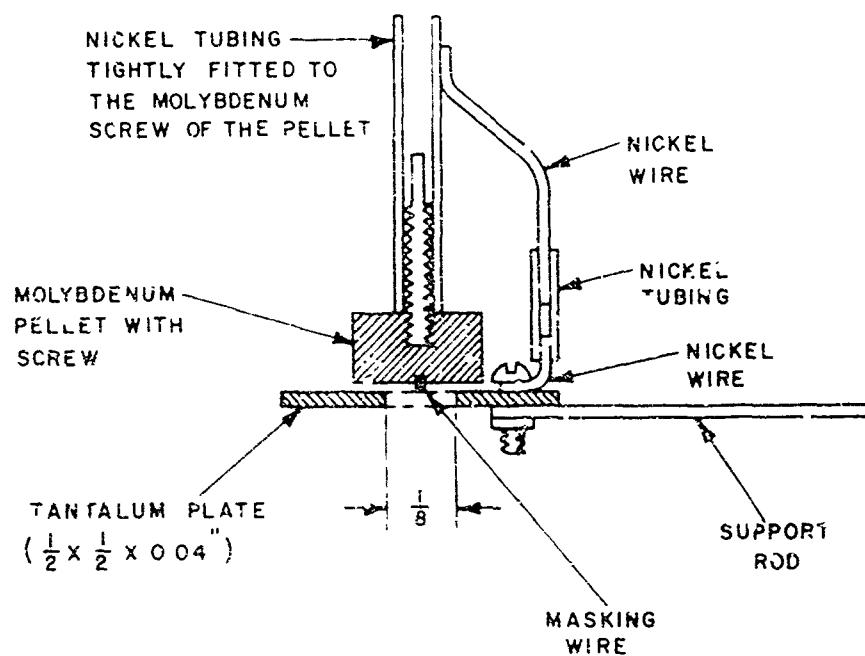


FIGURE 20. TRANSVERSE-FIELD CATHODES #9 THROUGH #11:  
ASSEMBLY OF THE MOLYBDENUM PELLETT  
AND THE TANTALUM MASK

external heat applied to the pellet. The basket temperature was gradually increased to a maximum of  $1440^{\circ}\text{C}$ . The deposition was completed within 35 minutes. The bell jar pressure was  $1 \times 10^{-7}$  torr. The thickness of the SiO deposit was 1 to 1.5 microns.

The top molybdenum film was deposited onto the sample through the mask previously described and shown in Figure 20 without prior degassing of the sample. An E-gun was used to evaporate the molybdenum. The molybdenum source was a pre-degassed pellet. The distance between molybdenum source and sample was 4". The molybdenum was evaporated at a temperature of about  $2000^{\circ}\text{C}$  and at a bell jar pressure in the low  $10^{-6}$  torr region. The deposition took place over a period of 20 minutes. The thickness of the molybdenum deposit was 2000 to 3000 Å. The deposit did not have the very shiny and smooth appearance of molybdenum films deposited on a microscope slide or sapphire substrate. The surface was rather coarse and grainy, but did not display obvious defects.

The removal of the nickel wire mask by hot hydrochloric acid (initially diluted, later more and more concentrated HCl) proved to be a lengthy process requiring approximately 4 hours for completion. But no apparent damage of the films was observed. Testing of the sample with a continuity meter, however, revealed a short circuit between the top molybdenum film and the molybdenum pellet. No electrical continuity was found when probing the bare region of the SiO layer against the bulk of the pellet. Microscopic examination of the sample (magnification 200X) showed several holes in the SiO layer, but these holes were probably formed during the acid treatment. There were also indications that the acid had etched the top molybdenum film here and there. Around the hole in the center of the sample, dark spots were observed. The nature of these spots could not be determined.

#### Transverse-Field Cathode # 10

Although there was no evidence that defects of the SiO layer were responsible for the failure of Cathode # 9,  $\text{Al}_2\text{O}_3$  was tried as insulating material in the preparation of Cathode # 10. A piece of "green" (unfired) alumina ceramic (99.5 %  $\text{Al}_2\text{O}_3$ ) was used as the  $\text{Al}_2\text{O}_3$  source. The heat source was an E-gun. The molybdenum pellet was located at a distance of 5" from the  $\text{Al}_2\text{O}_3$  source. Before outgassing the molybdenum pellet the  $\text{Al}_2\text{O}_3$  source was degassed by heating in forepump vacuum to a maximum temperature of  $1140^{\circ}\text{C}$  within 35 minutes. The  $\text{Al}_2\text{O}_3$  source was allowed to cool and the molybdenum pellet was degassed by heating in high vacuum ( $1 \times 10^{-6}$  torr) for 10 minutes at about  $1100^{\circ}\text{C}$  (heat-up time 40 minutes). After cooling of the molybdenum pellet, the  $\text{Al}_2\text{O}_3$  was heated until evaporation took place at a temperature of about  $2000^{\circ}\text{C}$  (heat-up time: 20 minutes). The shutter between the molybdenum pellet and the  $\text{Al}_2\text{O}_3$  source was removed and the deposition of the  $\text{Al}_2\text{O}_3$  onto the pellet performed within 1 hour and 10 minutes. The temperature of the  $\text{Al}_2\text{O}_3$  source climbed during the deposition to about  $2300^{\circ}\text{C}$ . The pressure in the bell jar was in the low  $10^{-6}$  torr region. The thickness of the  $\text{Al}_2\text{O}_3$  deposit was of the order of 1 micron. The deposit was finally aged by a brief heating at about  $1150^{\circ}\text{C}$ .

The sample was inspected and it was found that the masking nickel wire had melted. Apparently, alloying of the nickel with the

molybdenum had occurred indicating that the temperatures applied to the molybdenum pellet had been excessive. It was furthermore noticed that the  $\text{Al}_2\text{O}_3$  layer looked gray instead of white. Testing of the layer for its insulating quality showed that the  $\text{Al}_2\text{O}_3$  was highly conductive and therefore worthless. It was assumed that oxygen deficiency was the reason for the conductivity of the  $\text{Al}_2\text{O}_3$ . The sample was discarded.

#### Transverse-Field Cathode # 11

As in Cathode # 9, SiO was the insulator in Cathode # 11, but platinum was used instead of molybdenum as the top metal film material. Platinum was selected because of its high chemical inertness and greater volatility.

The molybdenum pellet was degassed for 30 minutes at temperatures between  $900^\circ$  and  $950^\circ$  (heat-up time: 15 minutes). The SiO was evaporated from the standard tungsten basket. The degassing and deposition of the SiO generally followed the procedures used in previous preparations of SiO layer; but an extra heavy deposit of 2 to  $2\frac{1}{2}$  micron thickness was formed in three separate runs. Tested with the continuity meter, the layer was found to be insulating.

The top platinum film was deposited through the mask used during the deposition of the top molybdenum film of Cathode # 9. The mounting of the mask was the same as shown in Figure 20, but the diameter of the circular opening of the mask was widened from  $1/8"$  to  $3/16"$ . The platinum source was a strip of sheet metal, 3 mils thick and  $1/4"$  wide, folded and pressed to a square package. An E-gun was used as heat source. The distance between platinum source and sample was 5".

The platinum source was degassed by raising the temperature to about  $1700^\circ\text{C}$  within 1 hour. At this temperature, the platinum started to evaporate (bell jar pressure  $1 \times 10^{-5}$  torr). The shutter between platinum source and sample is removed and the platinum deposited onto the sample to a thickness of 3000 to 4000 Å (deposition time: approximately 2 hours; final bell jar pressure:  $2 \times 10^{-6}$  torr).

Under vacuum, the platinum film appeared to be smooth and quite satisfactory, but immediately upon exposure to air, the film wrinkled. The adherence of the platinum to the SiO layer proved to be extremely poor. The slightest touch with a probe wire caused peeling. Except for a few specks, the entire film could be easily removed. The bare SiO layer appeared to be still insulating when tested with the continuity meter.

#### SUMMARY

##### A. Field-Emission Type of Cathodes

The formation of asperities has been demonstrated on plain molybdenum layers using the aluminum alloying technique. The various factors, such as quantity of aluminum, residual gas pressure, temperature and time of the heat treatments, that may control size and density of the asperities have not been investigated in detail. It has been only determined that too little aluminum fails to produce asperities whereas an excess of aluminum

results in irregular corrosion of the molybdenum surface.

Two experiments were performed in which asperities were grown on molybdenum areas confined by insulating layers. The areas were narrow grooves and were formed in layers of alumina and silicon monoxide, respectively, by evaporating the insulators through a nickel mesh grid onto the molybdenum layer. It was found that, in the experiment with silicon monoxide, the growth of asperities had spread across the entire width of the grooves whereas in the experiment with alumina, the asperities had formed primarily in the middle of the grooves. No asperities were present in the immediate vicinity of the insulating layer.

In a third experiment, an attempt was made to produce asperities on molybdenum within grooves etched in a silicon monoxide layer. The experiment had to be discontinued prematurely because of a failure in the production of the grooves.

#### B. Transverse-Field Type of Cathodes

The preparation of transverse-field cathodes has been explored using various cathode configurations, materials and techniques.

For producing the conductor, semiconductor and insulating layers of the cathode structures vacuum-deposition methods appeared to be superior to spray-coating techniques because of better control of the thickness and smoothness of the layers prepared by vacuum deposition. The use of metal foils as electrodes proved to be impractical primarily because of difficulties in making and maintaining reliable electrical contacts.

The use of masking wires for forming the gaps between the conductors was tried because of the simplicity of the method. For producing gaps sufficiently narrow to permit the use of moderate bias voltages for creating the required high electric fields across the gaps the masking wire technique was considered inadequate. The control of the gap width by an insulating layer sandwiched between the conductors was therefore explored as a more useful method. Difficulties were experienced from short circuits between the conducting layers. It appeared that this failure was not necessarily caused by defects of the insulating layer, but may have resulted in some instances from improper coverage of the critical edge of the base conductor by the insulating layer. Measures for eliminating this possible fault were indicated.

The feasibility of preparing a BaO film capable of carrying an electron current across the gaps has been demonstrated. The failure of drawing some of the electrons into vacuum was explained by the excessive width of the gaps.

Although the active area of most of the investigated cathode configurations was a straight edge, a special cathode structure was also explored in which the emission was to emerge from the wall of a circular hole. Several cathode samples were prepared, but so far with limited success.

## FUTURE PLANS

### A. Field-Emission Type of Cathodes

Thus far, the samples prepared in the various experiments have been evaluated only by microscopic inspection. This examination provided information on the number and size of the asperities, but did not permit evaluation of their geometrical shapes. According to the final objective of the program, the asperities are supposed to serve as field emitters. The shape of a field emitter is critical for its field emission characteristics and, therefore, very important. Electron microscopy would provide a tool for determining the geometrical shape of the asperities and, hence, offer an indication of their capabilities as field emitters, but the procedure is intricate and the information still limited. Since a modified Mueller field-emission microscope (4,5) that permits scanning of a surface by a small-size electrode was available in the Techniques Branch of the Laboratory it was decided to use this instrument for testing the asperities directly for their field emission characteristics. By comparing the field emission characteristics of different samples and correlating the results with the preparation conditions, guidance will be obtained in the formation of asperities with the most desirable characteristics. Because of the scanning feature of the instrument, it will also be possible to test the uniformity of the shape of the asperities across the surface of an individual sample.

The field emission microscope has been readied for operation and testing of one of the samples with asperities grown on plain molybdenum is imminent. Depending on the results, the future work will continue with the formation of asperities inside grooves in insulator layers or will return to the investigation of the growth of asperities on plain molybdenum. This return would be justified if the present asperities prove to be field emitters of such a poor quality that a more detailed study of their growth is necessary to achieve the required improvement. In this case, the formation of the asperities on plain molybdenum would simplify the experimental procedures.

### B. Transverse-Field Type of Cathodes

No further work is planned for this type of cathode.

#### REFERENCES

1. D. V. Geppert and B. V. Dore, "Transverse-Field Emitter", Eighth National Conference on Tube Techniques, 20 to 22 September 1966, New York City.
2. S. Cabell, D. Dobischek, "Preparation of Thin-Film Tunneling Structures", Technical Report ECOM-2718, August 1966.
3. C. Hartelius, W. W. Hansen, "Applied Research in Thin-Film Field-Emission Tubes", Technical Report ECOM-01766-6, May 1967, Sixth Quarterly Report, Contract DA 28-043 AMC-01766(E), Stanford Research Institute, Menlo Park, California.
4. H. Guetzlaff, H. Hieslmair, R. B. Rauch, "Progress Report on Further Work with the Special Field Emission Projection (Mueller) Microscope", Memorandum Report, Techniques Branch, U. S. Army Electronics Laboratory, Fort Monmouth, New Jersey (1965).
5. H. Hieslmair, "Studies of Field Emission and Electrical Breakdown Between Micron-Sized Areas," Technical Report ECOM-2583, March 1965.

#### ACKNOWLEDGEMENTS

Acknowledgement is made to Messrs. Mortimer H. Finn and Munsey E. Crost of USAECOM and Kenneth R. Shoulders of Stanford Research Institute who originated the concept of the scannable field-emission type of cathodes.

The authors further wish to express their appreciation to Mrs. M. Osborn, Techniques Branch, for her active and constant participation in solving many of the part fabrication and mounting problems, and to Messrs. H. Guetzlaff and C. LoCascio, Techniques Branch, for their ready and competent assistance in the modification of the vacuum station.

Unclassified

Security Classification

DOCUMENT CONTROL DATA R & D		
(Security classification of title, body, abstract and indexing annotation must be entered when the overall report is classified)		
1. ORIGINATING ACTIVITY (Corporate author)		2a. REPORT SECURITY CLASSIFICATION
U. S. Army Electronics Command Fort Monmouth, N. J.		Unclassified
3. REPORT TITLE		2b. GROUP
Techniques for Fabricating Scannable Cold Cathodes		N/A
4. DESCRIPTIVE NOTES (Type of report and inclusive dates)		
Technical Report		
5. AUTHOR(S) (First name, middle initial, last name)		
Dietrich Dobischek Nelson D. Dent		
6. REPORT DATE	7a. TOTAL NO. OF PAGES	7b. NO. OF REFS
March 1968	48	5
8a. CONTRACT OR GRANT NO.		8b. ORIGINATOR'S REPORT NUMBER(S)
a. PROJECT NO. LH6 22001 A 055		ECOM-2948
c. Task No. LH6 22001 A 055 03		9b. OTHER REPORT NO(S) (Any other numbers that may be assigned this report)
d. Subtask No. LH6 22001 A 055 03 34		
10. DISTRIBUTION STATEMENT		
This document has been approved for public release and sale; its distribution is unlimited.		
11. SUPPLEMENTARY NOTES		12. SPONSORING MILITARY ACTIVITY
		U. S. Army Electronics Command Fort Monmouth, N. J. 07703 AMSEL-KL-TD
13. ABSTRACT		
<p>A. Experiments with Field Emission Type of Cathodes. The formation of asperities has been demonstrated on plain molybdenum layers using the aluminum alloying technique. It was found that too little aluminum fails to produce asperities whereas an excess of aluminum results in irregular corrosion of the molybdenum surface. Experiments in which asperities were grown on molybdenum areas confined by insulating layers showed that the presence of these layers may affect the formation of asperities. Alumina inhibited the growth of asperities in the immediate vicinity of the alumina layer. Silicon monoxide did not appear to adversely influence the formation of asperities.</p> <p>B. Experiments with Transverse-Field Type of Cathodes. The preparation of transverse-field type of cathodes has been explored using various cathode configurations, materials and techniques. Vacuum deposition methods were found to be superior to spray-coating techniques in the preparation of the cathodes. Cathode configurations in which the gap between the two conductors was controlled by an insulating film sandwiched between the conductors appeared to be the most promising approach toward the fabrication of a useful cathode. Difficulties were experienced with such structures from short circuits between the conducting layers. It was concluded that these failures were not necessarily caused by defects of the insulating layer, but that, in some instances, the two conductors may have come in direct contact inside the structure due to a mismatch of the thicknesses of the insulating layer and the base electrode. The feasibility of preparing a BaO film such as to carry an electron current across the gap of a cathode structure has been demonstrated.</p>		

DD FORM 1473

REPLACES DD FORM 1473, 1 JAN 64, WHICH IS OBSOLETE FOR ARMY USE.

(1)

Unclassified

Security Classification

Unclassified  
Security Classification

14. KEY WORDS	LINK A		LINK B		LINK C	
	ROLE	WT	ROLE	WT	ROLE	WT
Field-emission cathodes Asperities Transverse-Field Cathodes Vacuum deposition methods						

ESC-FM 2033-68

(2)

Unclassified  
Security Classification